EMEP/CCC-Report 4/2002

EMEP Co-operative Programme for Monitoring and Evaluation of the Long-Range Transmission of Air Pollutants in Europe

Measurements of Particulate Matter: Status Report 2002

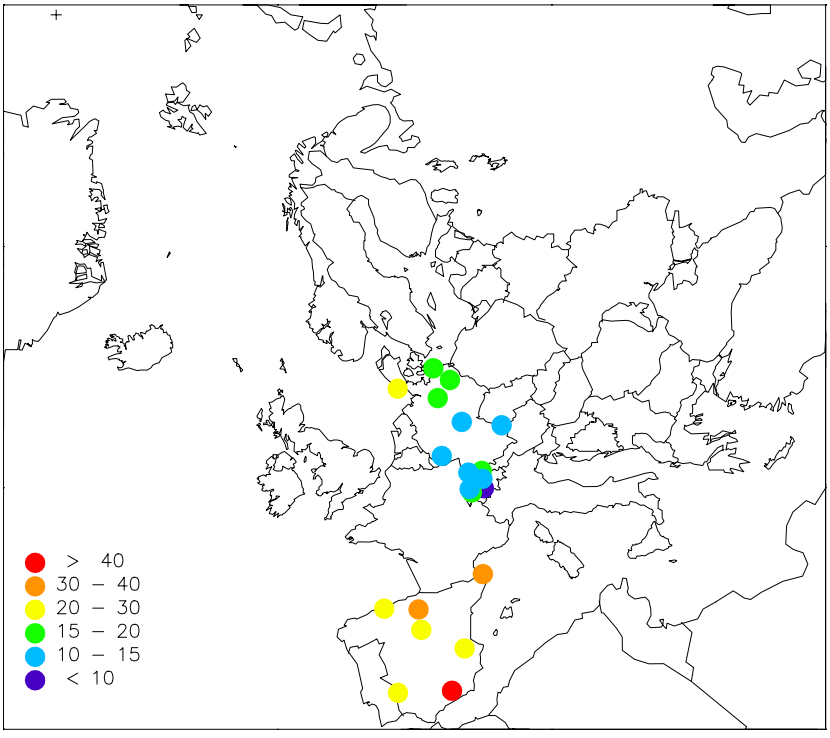

Norwegian Institute for Air Research
PO Box 100, NO-2027 Kjeller, Norway
Chemical Co-ordinating Centre of EMEP (CCC)

NILU : EMEP/CCC-Report 4/2002
REFERENCE : O-98134
DATE : AUGUST 2002

EMEP Co-operative Programme for Monitoring and Evaluation of the Long-range Transmission of Air Pollutants in Europe

Measurements of Particulate Matter: Status Report 2002

Edited by Michael Kahnert

Norwegian Institute for Air Research
P.O. Box 100, N-2027 Kjeller, Norway

Contents

Page

Measurements of Particulate Matter: Status Report 2002

1. Introduction

M. Kahnert
Norwegian Institute for Air Research, P.O. Box 100, 2027 Kjeller, Norway

The objective of the EMEP monitoring programme is to attain a better characterisation of air pollutant concentrations in Europe, their emission, composition, transformation, transport, and deposition in relation to human health and air quality standards. Another goal is to validate chemical transport models, which are essential tools for predicting the effects of emission changes and to develop cost-efficient abatement strategies. The emphasis in the EMEP monitoring programme is on the long-range transport of air pollutants. Use of monitoring data to investigate the cause-effect relationship between emissions and air quality is of primary importance with regard to validating the effectiveness of emission control policy measures for improving air quality.

Monitoring of aerosol particles is a relatively recent addition to EMEP that was included in the programme in 1999. Particles in air are suspected to be a major contributor to the adverse short- and long-term effects on human health associated with air pollution. Epidemiological studies suggest that particulate matter (PM) can cause cough and respiratory peak flow reductions, alveolar inflammation (Pope et al., 1995), cardiovascular effects by induced changes in blood coagulability (Seaton et al., 1995), and increased morbidity and mortality (Pope et al., 1995; Dockery et al., 1995; Pope et al., 1995). Toxicological studies corroborate the epidemiological evidence for the negative effects of PM on human health (Schlesinger, 1995). However, in contrast to most other pollutants, currently available data from epidemiological studies do not allow us to identify a threshold concentration of PM below which no adverse health effects occur (WHO, 2000). Thus comprehensive long-term investigations are required to attain a better understanding of the exposure of people to particulate pollutants and the resulting consequences for human health.

The high relevance of PM for human health necessitates abatement policies, of which the successfulness needs to be validated by both measurements and model calculations of PM concentrations. This is the main motivation for including PM long-term monitoring into EMEP. As the relevant quantity to be monitored the EMEP programme has chosen the mass concentration of PM in air with an aerodynamic equivalent diameter of less than 10 μm, denoted by PM_{10}, and measured in $\mu g/m^3$. This choice is in accordance with EU monitoring standards. Particles with an aerodynamic diameter of more than 10 μm cannot penetrate deeply into the human respiratory tract. For this reason they are not considered to be relevant for adverse respiratory health effects. However, accumulating evidence suggests that $PM_{2.5}$, sulphate, and strongly acidic constituents of $PM_{2.5}$, or oven smaller mass fractions such as $PM_{1.0}$ may better serve as predictors of health effects than PM_{10} (WHO, 2000). It is therefore conceivable that current

abatement policies and monitoring strategies will have to be revised and amended in the future.

The chemical composition and physical properties of aerosols contain information about the particles' sources. These properties also determine the aerosols' interaction with the human respiratory system, but also the transport, transformation, and deposition of particles. Aerosols can be classified according to their origin as either primary or secondary, or as natural or anthropogenic. Secondary aerosols originate from homogeneous or heterogeneous chemical reactions of precursors or by photochemical mechanisms (Pandis et al., 1991). Typical precursor gases are sulphur dioxide, nitrogen oxides, ammonia, and volatile organic compounds (VOC). The precursors can be of natural or anthropogenic origin, where the latter are usually predominant in Europe. The precursor gases can form particles either by homogeneous nucleation, by condensation onto existing particles, or by chemical and photochemical reactions. Primary natural aerosols originate from sea spray (salt aerosols) (Savoie and Prospero, 1982), soil resuspension by wind (Nicholson, 1988) (e.g. Saharan dust (Rahn et al., 1979)), or volcano emissions (Haulet et al., 1977). The most important anthropogenic sources of aerosols or precursor gases of secondary particles are road transport, combustion sources, fossil fuel power plants, and agriculture.

This report presents EMEP monitoring data of particulate matter in air for the year 2000. The current status of the EMEP monitoring work with regard to PM is reviewed, and envisaged extensions of EMEP activities in this field – both geographical and concerning the sort of measurements being conducted – are discussed. More comprehensive monitoring information is needed on physical and chemical properties of particles in air in order to attain a more complete picture of these complex pollutants. The contribution of elemental and organic carbon (EC/OC) species to the total aerosol mass is presently one of the most important issues. The EC/OC campaign within the EMEP network and its methodical approach are introduced in this report. The potential enhancement of our understanding that can be gained from comprehensive measurements is exemplified by the presentation of two different research campaigns that were conducted in the year 2001 in Norway and Greece, respectively.

2. PM_{10} measurements within EMEP

M. Kahnert, K. Tørseth, A.-G. Hjellbrekke, W. Aas, and J. E. Hanssen
Norwegian Institute for Air Research, P. O. Box 100, 2027 Kjeller, Norway

In 2001 at its 25th session the EMEP steering body adopted the PM monitoring strategy of which a detailed description can be found at www.nilu.no/projects/ccc/pm_strategy.html. At the third meeting of EMEP's task force on measurements and modelling (TFMM) in March 2002 the revised draft of the EMEP Manual for Sampling and Chemical Analysis (EMEP/CCC, 1996) for PM_{10} mass measurements and chemical speciation was adopted. The mass measurement part is based on standard EN 12341 of the European Committee for Standardization (CEN) (CEN, 1998) and recommends employing the gravimetric method, which has proven to be the most accurate method. Gravimetric methods also have the advantage of allowing chemical analysis of the collected PM_{10} sample after weighing. The applications of methods and quality assurance procedures recommended by the manual is important in order to harmonise the ongoing PM_{10} measurements (EMEP, 2001; Lazaridis et al., 2002) throughout the EMEP network.

Nevertheless, there is different measurement equipment presently in use, which is a challenge for quality assurance. It should be noted that parties can decide to use sampling equipment other than the high- or low-volume reference samplers listed in the EMEP manual, provided that their sampling equipment has been demonstrated to give results comparable to those obtained with the reference methods.

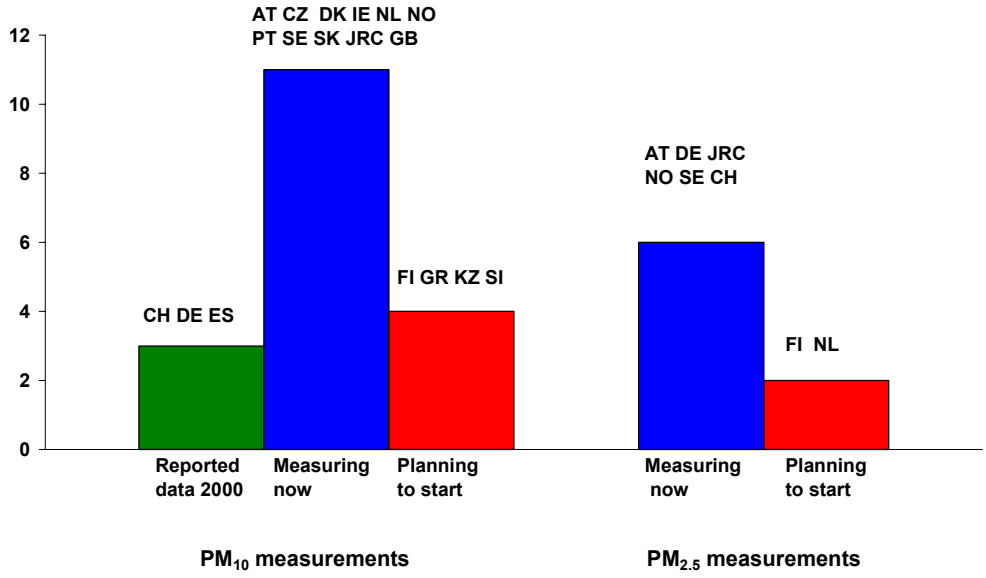

Figure 1: Number of countries measuring PM_{10} and $PM_{2.5}$.

As illustrated in Figure 1 only three countries have reported PM_{10} data in the year 2000 from a total of 26 stations (five Swiss, eight German, and 13 Spanish stations). However, it is expected that the number of stations will double in the near future, and that the spatial coverage of Europe will improve substantially. In

2002, Austria, the Czech Republic, Denmark, Ireland, the Joint Research Centre (JRC) in Ispra (Italy), The Netherlands, Norway, Portugal, Sweden, Slovakia, and Great Britain were measuring PM_{10} in addition to Switzerland, Germany, and Spain. In the near future, PM_{10} monitoring is also expected to start in Finland, Greece, Slovenia, and possibly in Kazakhstan. Table 1 provides an overview over stations and measurement equipment in different European countries. Not all the collected data have been reported to EMEP-CCC.

Table 1: List of countries measuring PM_{10}, and of equipment used.

Country	Stations meas. PM_{10}	start measuring	Time resolution	Instrument
Austria	AT02 AT04 and AT05	Jul. 1999 Jan. 2001	daily	Digitel High Vol. DHA80
Belgium				
Croatia				
Czech Republic	CZ01 and CZ03		30 min	radiometry (Verewa)
Denmark	DK05	Oct. 2001	24h	SM200 (ADAM)
Estonia				
Finland	FI04 or FI17	Spring 2002	daily	Kleinfiltergerät
France				
Germany	DE01, 02, 03, 04, 05, 07, 08, 09	1 Jan. 1999	daily	Digitel High Vol. DHA80
Greece	GR1, Aliartos	Autumn 2003		not decided
Hungary				
Iceland				
Ireland	IE31 Mace Head	Aug. 2001	daily	U Miami Hi Volume
Italy (IT1)				
JRC -Ispra	IT04	Mar. 2000	daily	Kleinfiltergerät
Kazakhstan	Borovoe	Jan. 2003		SKC or Casella
Latvia				
Lithuania				
Macedonia	no			
Moldovia	no			
Netherlands	NL09 and NL10	1992/93	hourly	beta-dust FH 62 I-N
Norway	NO01	Jan. 2000	daily	Kleinfiltergerät
Poland				
Portugal	PT03 and PT01	Since 1979	daily	HiVol, Sierra Andersen
Russia				
Slovakia	SK04	Oct. 2001	weekly	Partisol Plus R&P
Slovenia	SI03	2003	daily	Kleinfiltergerät
Spain	ES01, 03, 04, 05, 06, 07, 08, 09, 10, 11, 12	1997	daily	MCV
Sweden	SE12	Mar. 1990	24 h (particles)	R&P ACPM and
	SE11 and SE35	Sep. 99 and Jan. 02	1h, 3h and 24 h	R&P TEOM
Switzerland	CH01, 02, 03, 04, 05	Jan. 1997	daily (48h CH01)	Digitel high vol. DHA80
Turkey				
UK	UK43 and UK06	1997	hourly	
Yugoslavia				

Figure 2 shows annual averages of PM_{10} concentrations measured in 2000 for different countries. The data are from EMEP and from the AIRBASE database operated by the European Topic Centre on Air and Climate Change (ETC/ACC) under contract of the European Environmental Agency (EEA)[1]. The data shown have been obtained by averaging for each country over all stations that reported PM_{10} data in that country. Site locations and other factors make direct comparisons of concentration levels difficult. All reporting stations have been included into the average regardless of their temporal data coverage. EMEP-data are represented by blue columns. The AIRBASE results represent PM_{10} data from rural (green), urban (red), and traffic (black) sites. Due to the large number of different methods employed in obtaining the AIRBASE data, the results are mainly meant to indicate qualitative trends. Also indicated in the figure is the indicative value according to the EU directive of an annual PM_{10} concentration average of 40 µg/m^3 for the target year 2005 (dotted line), and the corresponding indicative value of 20 µg/m^3 for the target year 2010 (dashed line).

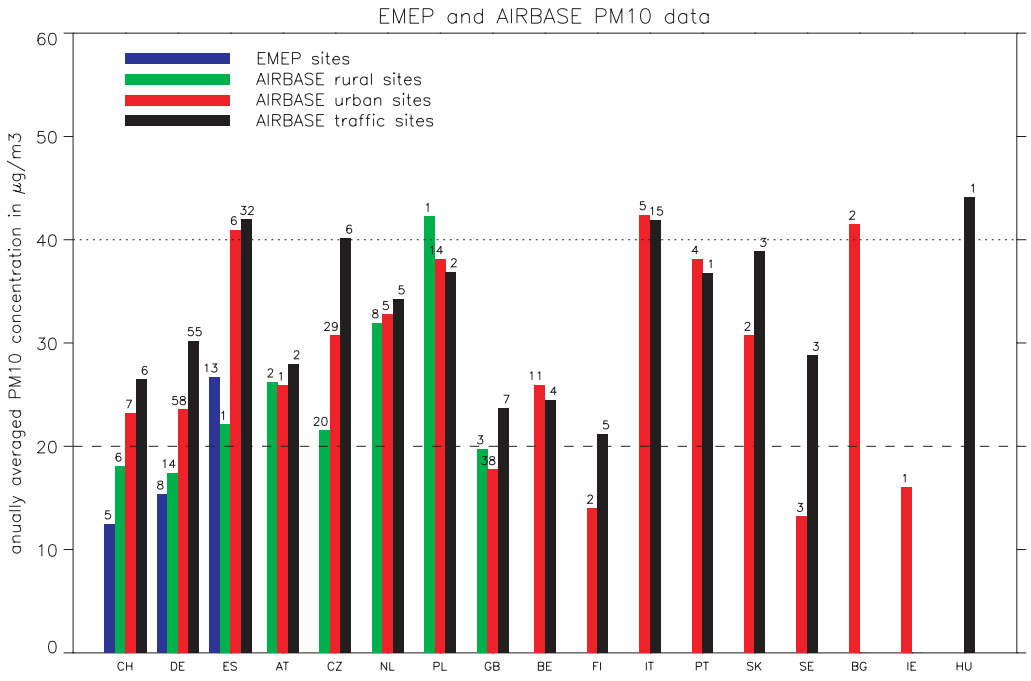

Figure 2: Annual and country-averages of PM_{10} concentrations at EMEP background sites (blue), and at rural (green), urban (red), and traffic sites (black) in 2000. Numbers over each column indicate the number of stations over which the country-average has been taken. The data for rural, urban, and traffic sites have been extracted from the AIRBASE data base.

Figure 2 shows for some countries rather small differences in PM_{10} concentrations between urban and rural sites. Even though local sources in urban centres or agricultural sources in rural areas can be important contributors to the observed PM_{10} concentrations, a significant contribution usually originates from aerosols

[1] AIRBASE data have been extracted by F. de Leeuw (RIVM, The Netherlands).

that have been transported over regional scales. This results in small differences between the time-averaged PM_{10} concentrations observed at urban sites and at rural background sites. The annually averaged PM_{10} concentrations in Figure 2 are for most countries still far above the limit value set for 2010, in many cases even twice as high as the limit value.

Annual averages of PM_{10} concentrations measured at the different EMEP stations during 2000 are presented in Figure 3. Only those stations that have a data coverage of more than 50% are shown. This leaves only seven out of 13 Spanish stations. The full time-series of 24-hour PM_{10} concentrations measured at the different EMEP sites are presented in the Appendix. Figure 4 shows annual averages of PM_{10} concentrations at the different rural stations included in AIRBASE. Figure 5 and Figure 6 show corresponding results for urban and traffic sites[2]. Annual averages are based on concentrations measured over a 24 hour sampling period.

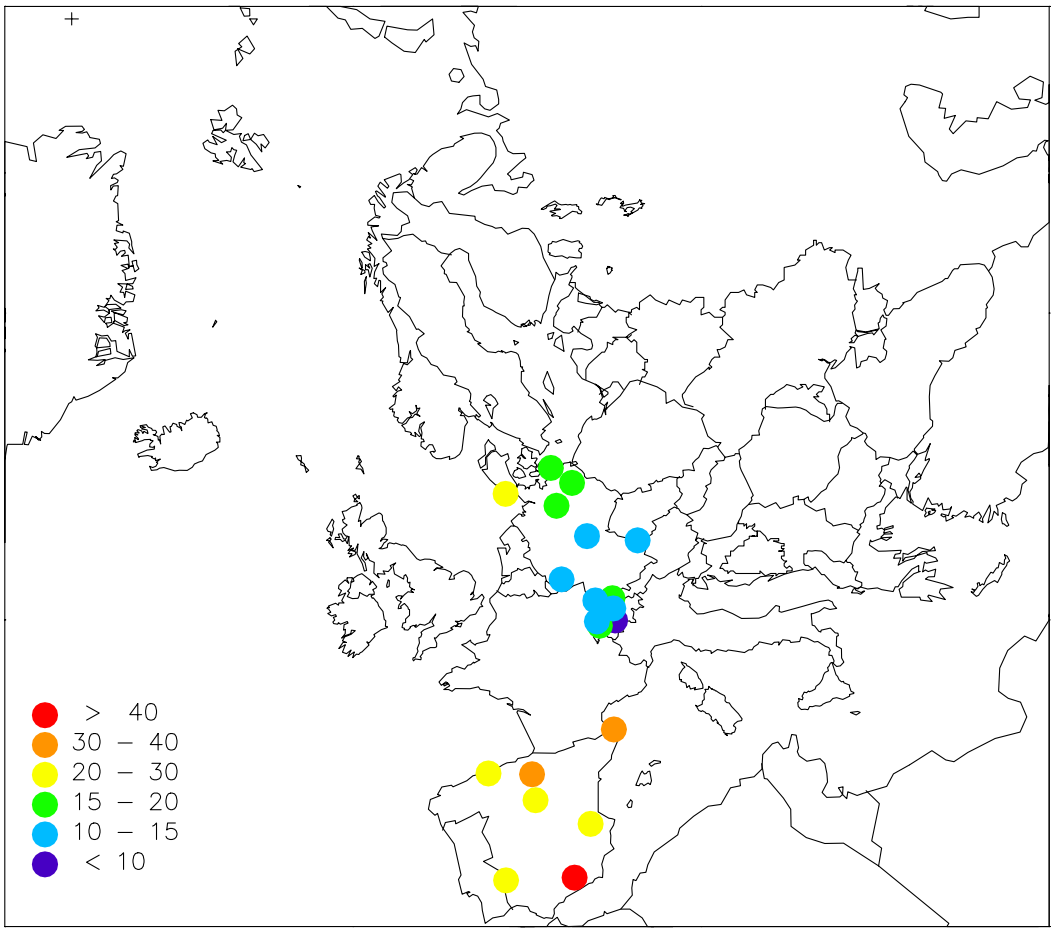

Figure 3: Annual averages of PM_{10} concentrations at EMEP sites in 2000 in $\mu g/m^3$.

[2] Figures 4–6 were produced by P. Kurfurst and J. Fiala (Czech Hydrometeorological Office).

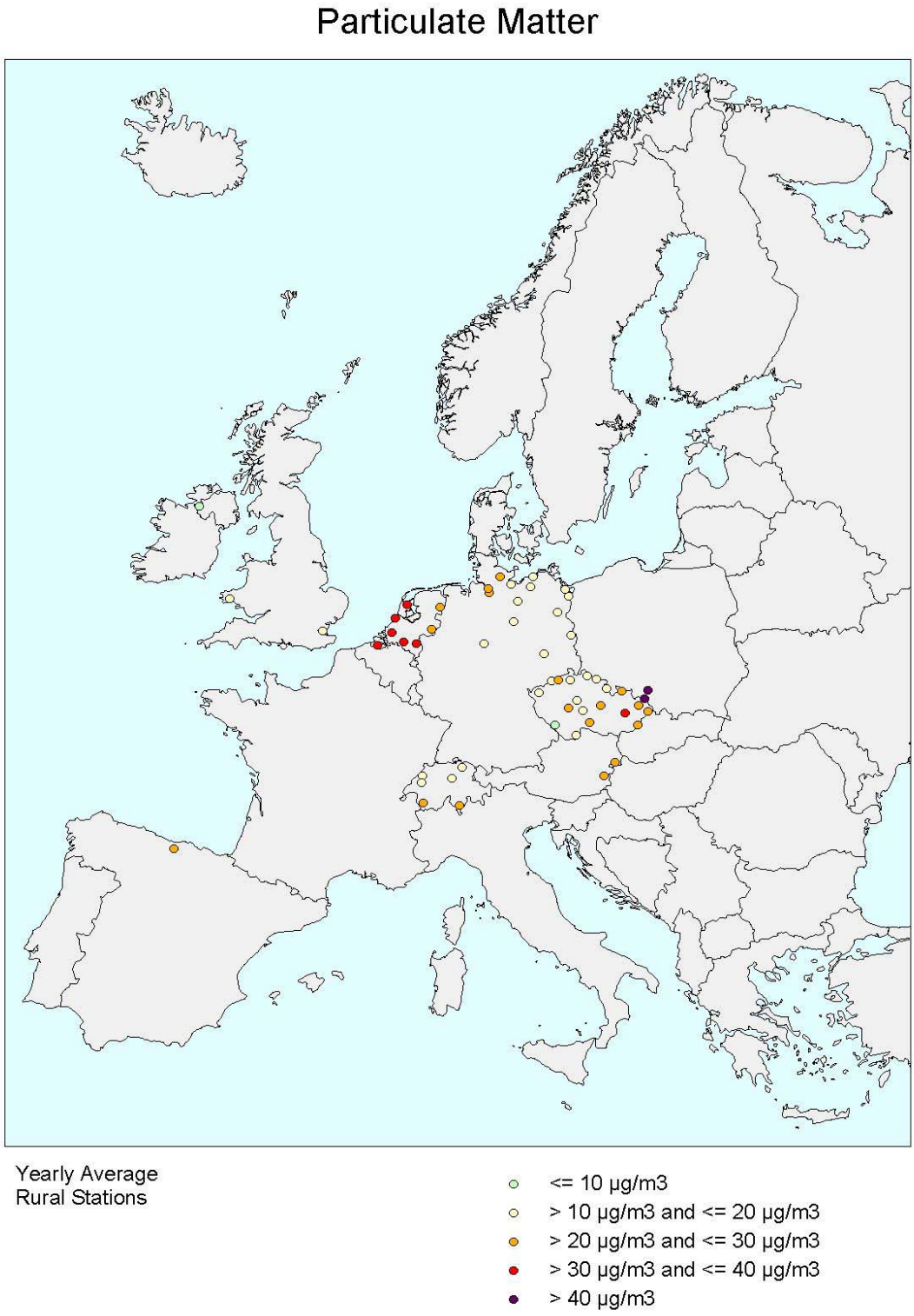

Figure 4: Annual averages of PM_{10} concentrations at AIRBASE rural sites in 2000.

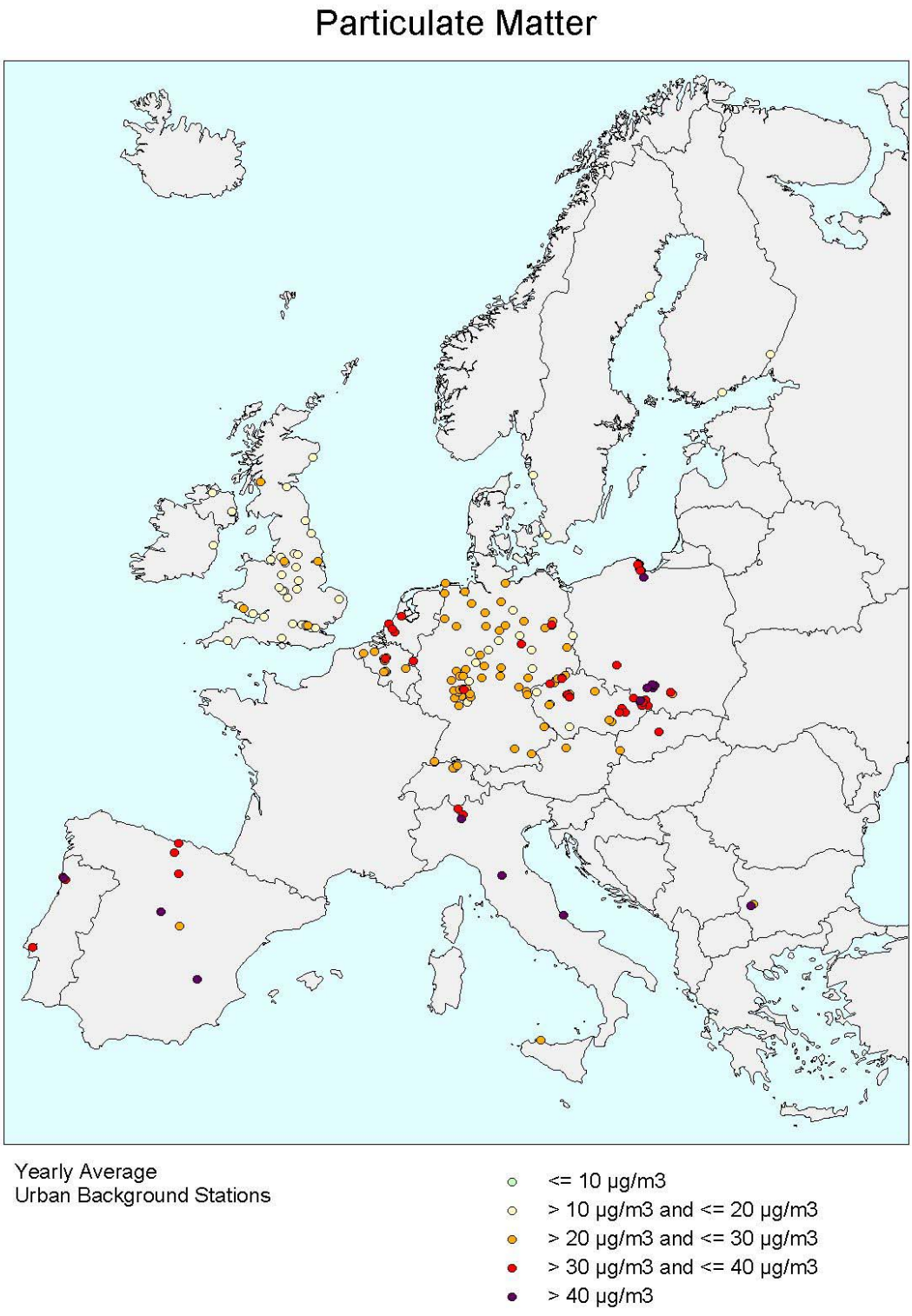

Figure 5: As Figure 4, but for AIRBASE urban sites.

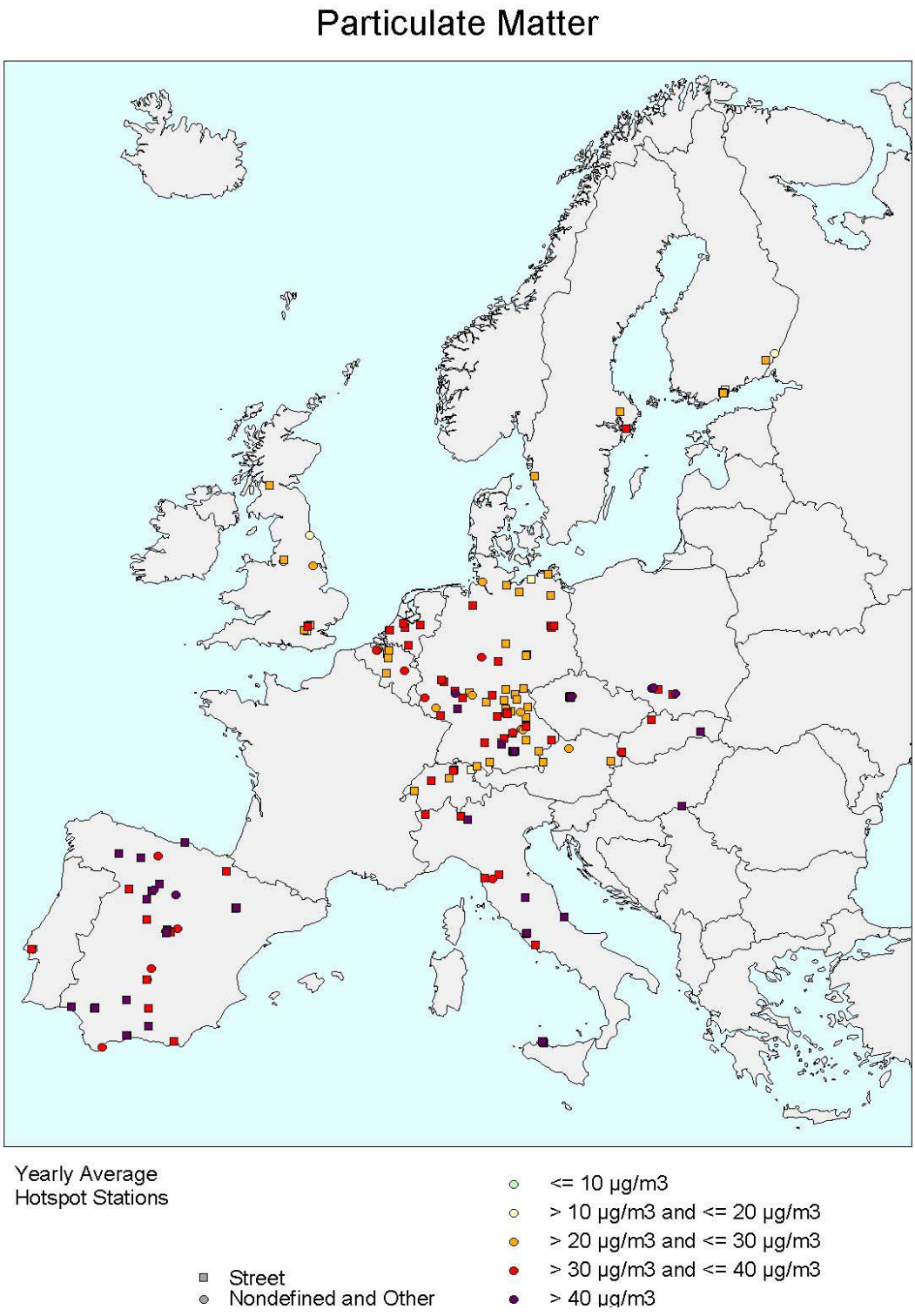

Figure 6: As Figure 4, but for AIRBASE traffic sites.

As mentioned earlier, PM_{10} monitoring has not proven to be sufficient for answering the relevant questions concerning the formation and behaviour of particulate matter in the atmosphere. More information about the physical and chemical properties of aerosols is needed, which places additional requirements on the monitoring programme. The PM strategy thus requires monitoring of other parameters to complement the measurements of PM_{10} mass. More specifically, a three-level approach has been adopted by the EMEP steering body. Level 1 activities shall consist of PM_{10} measurements that at least one station in each country will perform on a daily basis. In addition, a number of sites will send once a week samples to a common laboratory for the purpose of determining the fraction of elemental carbon (EC) and organic carbon (OC). Also, PM mass of fine particles ($PM_{2.5}$ and $PM_{1.0}$) as well as the concentrations of sulphate, nitrogen species, and base cations are to be measured at level 1 sites. Gas/particle distribution for nitrogen species using "artefact-free" methods, mineral dust analysis, and chemical speciation as a function of particle size shall be conducted at a limited number of sites (level 2 sites). At level 3 sites it is envisaged to undertake or make use of research campaigns or other advanced research activities usually not available at EMEP sites, such as OC-characterisation, measurement of number and area size distribution, light scattering measurements, determination of aerosol optical depth, etc.

Figure 7 provides an overview over the number of countries occasionally or routinely conducting more detailed aerosol studies at certain sampling sites (in 2002) and over the kind of measurements.

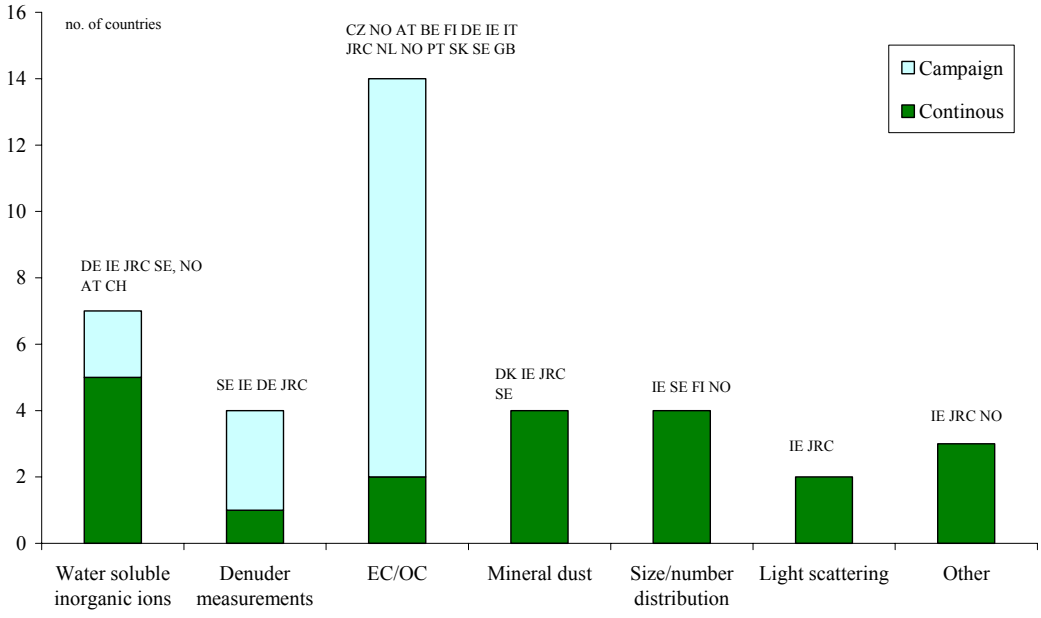

Figure 7: Overview over various aerosol measurement activities in different countries in 2002.

Elemental and organic carbon can constitute a significant portion of the total aerosol mass. However, this fraction is currently the most severe limitation of our ability to obtain mass closure for aerosols. Therefore a more accurate

determination of the EC/OC fraction is presently of high priority. Accounting for both organic and inorganic constituents of aerosol particles in models is also essential for accurately describing the physical and chemical processes in clouds and aerosols (Jakobsen et al., 2000). However, our knowledge about sources and composition of the EC/OC fraction of aerosols is still highly incomplete. Fossil fuel combustion (in the northern hemisphere) and biomass burning seem to be the major anthropogenic sources of OC. Oxidation of volatile organic compounds (VOC) is another, however poorly quantified source of OC. Very little is known about the impact of natural biological and marine sources. Due to the high significance of the EC/OC fraction of aerosols, a one-year EC/OC campaign within the EMEP network has been launched in the summer of 2002. In the future EMEP activities in this field are likely to be intensified. More details about the EC/OC campaign are provided in Sec. 3. In Section 4 results from a one-year research study at the EMEP site in Birkenes are presented concerning chemical characterization of PM_{10} and $PM_{2.5}$ particles. Section 5 presents results obtained from a measurement campaign in the eastern Mediterranean area.

3. EC/OC determination

C. Dye
Norwegian Institute for Air Research, P. O. Box 100, 2027 Kjeller, Norway

3.1 Introduction

Particulate matter (PM) is a very complex pollutant, and its mass includes a mixture of many chemical species distributed at different sizes. The concentrations of inorganic compounds are only to some extent well described across Europe. Sulphur and nitrogen compounds, which typically are those parameters that are determined at most EMEP sites, contribute between 20-50% to the aerosol mass. The chemical composition of the remaining mass is largely unknown. Carbonaceous material contributes significantly to this unknown fraction. In connection with the implementation of the EMEP monitoring strategy for particulate matter (see www.emep.int) an EC/OC measurement campaign has been launched in June 2002.

It is important to note that the determination of EC and OC is subject to many uncertainties and artefacts. This campaign will try to utilize the experiences gained through various research activities while at the same time taking a relatively simple and straightforward approach.

3.2 Objectives

The main objective is to provide information on ambient concentrations of organic carbon and elemental carbon for PM_{10} at a selection of sites across Europe. Sites have been selected by considering the sampling methodology applied, site representativity, and location (Table 2). The campaign is planned to last for one year.

Table 2: List of participants of the EC/OC-campaign.

Stations		Contact persons	Instrument/ Impactor	Filter size	Flow rate
AT02	Illmitz	Jürgen Schneider; Marina Fröhlich	Partisol	47 mm	16.7 l/min
BE	Univ. of Gent	Willy Maenhaut	Gent	47 mm	17 l/min
FI17	Virolahti	Minna Aurela; Risto Hillamo; Jussi Paatero		47 mm	38 l/min
DE02	Waldhof	Elke Bieber	HiVol (Digitel)	150 mm	500 l/min
IE31	Mace Head	Micheal Young; Gerard Jennings	KFG	47 mm	38 l/min
IT04	Ispra	Jean-Philippe Putaud	KFG	47 mm	38 l/min
IT	Belogna	Maria Cristina Facchini	Gent	47mm	17 l/min
NL09	Kollumerwaard	Ton van der Meulen; Dick van Lith	KFG	47 mm	
NO01	Birkenes	Jan Erik Hanssen	KFG	47 mm	38 l/min
PT01	Braganza	Renato Antero Carvalho	HiVol (Sierra)	8x10 inch	1133 l/min
SK04	Stara Lesna	Marta Mitosinkova	Partisol	47 mm	16.7 l/min
SE12	Aspvreten	Hans-Christen Hansson; Hans Areskoug	Gent	47 mm	15-18 l/min
UK	Edinburgh	J Neil Cape	Partisol	47 mm	16.7 l/min

3.3 Sampling

To assure data quality, the EMEP Manual for Sampling and Chemical Analysis (EMEP/CCC, 1996) for PM_{10} measurements and chemical speciation recommends the following standard procedures for EC/OC sampling.

Preparation of filters by NILU:

- Quartz filters from the same company will be used, however various sizes need to be prepared depending on the instrumentation of the participating countries (e.g. 47 mm, 140–150 mm, 8 x 10 inch).
- The filters are pre-heated to desorb possible OC on the filters and thereby minimise the blank values
- The filters are equilibrated (20oC, 50 % RH for 48h), weighed, and packed in transport containers.
- Each month four filters together with one blank are sent to the various contact persons.

At the field site:

- The duration of the campaign is one year, and the sampling frequency is once a week with 24 hours measurement periods, from 0800 local time Tuesday morning to 0800 Wednesday morning.
- The standard operational procedure varies from instrument to instrument and should therefore generally follow the different manufacture's instructions.
- The filters should be stored in a refrigerator in the transport containers until exposure.
- Always use tweezers when handling the filters. If one has to touch the filters always use anti-static powder free gloves.
- Inspect the filter for any pinholes, irregularities etc. Record the selected filter identification on a field log sheet. Insert the filter and bear in mind that the filters have an up side.
- Record the flow-rate before and after exposure or read the total flow if this is given. Record any unusual events, i.e. power brake down, storm, fires etc.
- After exposure, the high volume filters are first folded in two with the exposed sides against each other, while the low volume filers are placed directly in the transport container and sent to NILU. The field log sheet is sent together with the filters (please keep a copy of the form).

After the filters are returned to NILU:

- The filters are equilibrated (20oC, 50 % RH for 48h) and then weighed to determine the PM10 mass.
- EC/OC analysis will be performed.
- The major inorganic ions will probably also be measured.
- Some samples (parts of the same filters) will also be sent to the Finnish Meteorological Institute and the University of Gent for comparison of analytical methods.

3.4 EC/OC analysis

Thermal/optical EC/OC analysis is performed using an instrument from Sunset Laboratory Inc. (see Figure 8). A standard sized punch is taken from the exposed filters and placed in a quartz oven. The oven is purged with helium, and a stepped temperature ramp increases the oven temperature to 870ºC, thermally desorbing organic compounds and pyrolysis products into an oxidizing oven. The organic carbon is quantitatively oxidized to carbon dioxide gas. The carbon dioxide gas is mixed with hydrogen and the mixture subsequently flows through a heated nickel catalyst where it is quantitatively converted to methane. The methane is quantified using a flame ionisation detector (FID). After cooling the oven to 600ºC a second temperature ramp is initiated and the elemental carbon is oxidized off the filter by introducing a mixture of helium and oxygen into the oxidizing oven. The elemental carbon is detected in the same manner as the organic carbon (Birch et al., 1996; NIOSH, 1994). A schematic view of the observed thermogram is shown in Figure 9.

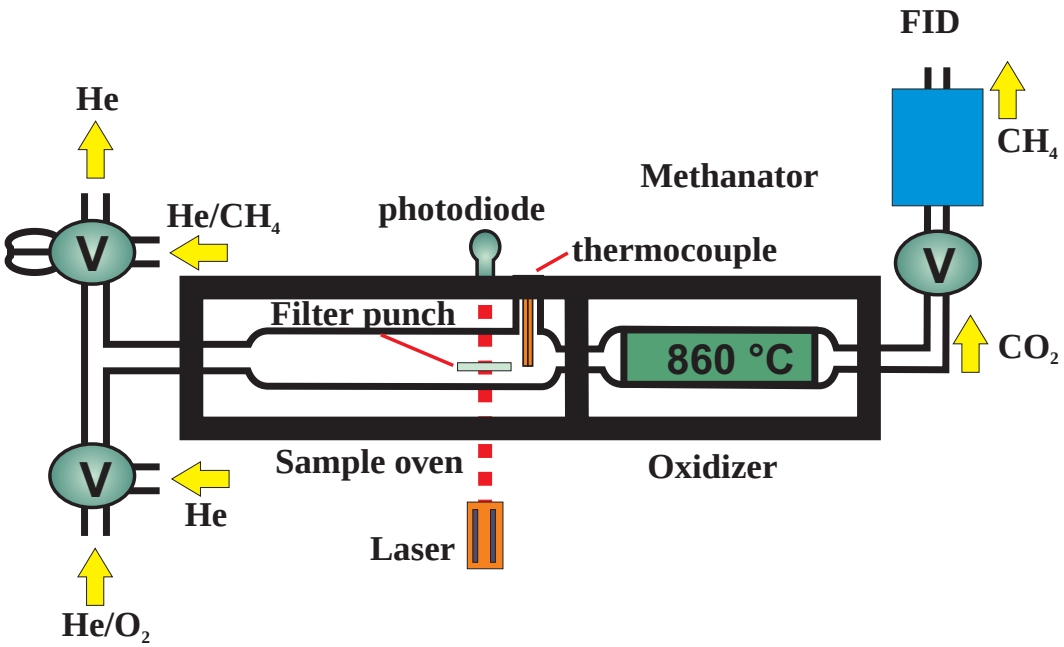

Figure 8: Schematic diagram of the Thermal-Optical Instrument (V=valve) (Sunset laboratory).

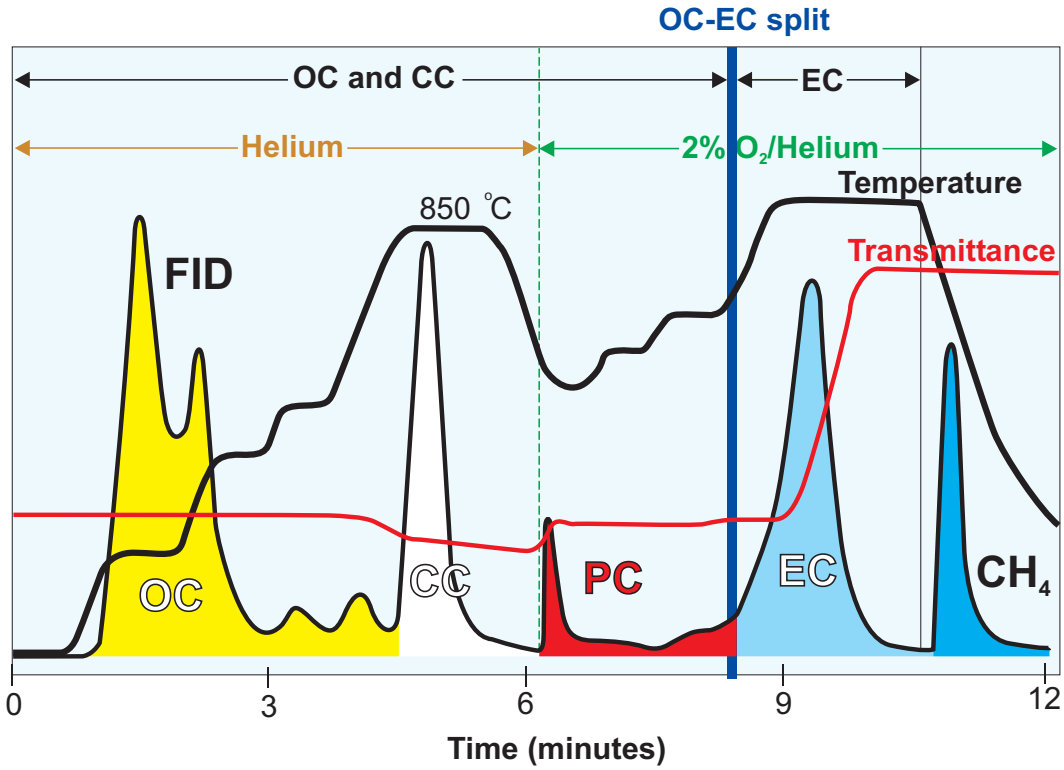

Figure 9: Thermogram for filter sample containing organic carbon (OC), carbonate (CC), and elemental carbon (EC). PC is pyrolytically generated carbon or 'char.' The final peak is the methane calibration peak. Carbon sources: pulverized beet pulp, rock dust (carbonate), and diesel particulate (Sunset Laboratory).

Comprehensive results for the EC/OC content of the PM_{10} samples collected weekly at the EMEP sites participating in the one-year campaign will be presented in 2003.

4. Chemical characterisation and mass concentration of ambient aerosol at the EMEP site in Birkenes (Southern Norway) – A one-year study

K. E. Yttri and K. Tørseth
Norwegian Institute for Air Research, P. O. Box 100, 2027 Kjeller, Norway

4.1 Introduction

A one-year research study has been conducted at the EMEP site in Birkenes (Southern Norway). Both PM_{10} and $PM_{2.5}$ mass concentrations have been measured, and the chemical composition of PM has been investigated.

Quantification of the PM_{10} mass fraction was included in the EMEP programme in 1999. Starting in 2000 sampling at Birkenes was performed using the Rupprecht & Patashnick Dichotomous Partisol-Plus model 2025, which samples both PM_{10} and $PM_{2.5}$, using Teflon filters (Pall Gelman Zefluor, 47 mm) conditioned for 48 hours at 20°C and at 50% RH before and after exposure. For quantification of elemental- (EC), organic- (OC) and total carbon (TC), weekly samples (7 days) were taken using two Small Filter Devices LVS 3.1 that collect aerosols with an equivalent aerodynamic diameter (EAD) of 2.5 μm and 10 μm (50% cut-off), respectively. Both instruments use quartz fibre filters (Whatman Q-MA, 47 mm) that were preheated for 2 hours at 800°C and then conditioned for 48 hours before and after exposure, thus being subjected to the same conditions as the Teflon filters.

Quantification of EC, OC and TC was performed using evolved gas analysis (Thermo Optical EC/OC method, Sunset laboratories Inc.). Data on inorganic compounds (sulphate, nitrate, ammonium, base cations and sea-salts), analysed by ion chromatography, were available from filter pack samples. The filter packs were not operating using a PM_{10} pre-impactor. However, the TSP- and PM_{10}-fraction are highly correlated at Birkenes.

4.2 Results and discussion

Mass concentration levels of PM_{10} are typically within the range of 5-8 μg m^{-3} (Figure 10) with an average of 6.0 μg m^{-3} (Table 3) for the entire sampling period. However, during episodes with air passing important source areas on the European continent mass concentrations on the order of 20-30 μg m^{-3} are seen (exemplified in Figure 11). Thus the air quality at Birkenes meets the guidelines set by the EU for PM_{10} [50 μg m^{-3} as a 24h mean, not to be exceeded on more than 35 days (indicative value for 2005) or on 7 days (indicative value for 2010)]. However, the data show that the regional contribution of PM_{10} may contribute up to 60% of the limit value in Southern Norway. The PM_{10} fraction can be divided into a fine and a coarse mode, designated by $PM_{2.5}$ and $PM_{10-2.5}$, respectively. The $PM_{2.5}$ mass concentration shows a relatively high correlation with the PM_{10} values and typically contributes 50-80% to the total PM_{10} mass concentration. The average $PM_{2.5}$ mass concentration for the sampling period is 4.0 μg m^{-3}. The coarse fraction, obtained by subtracting $PM_{2.5}$ from $PM_{10,}$ has an average of 1.9 μg m^{-3} (Table 3).

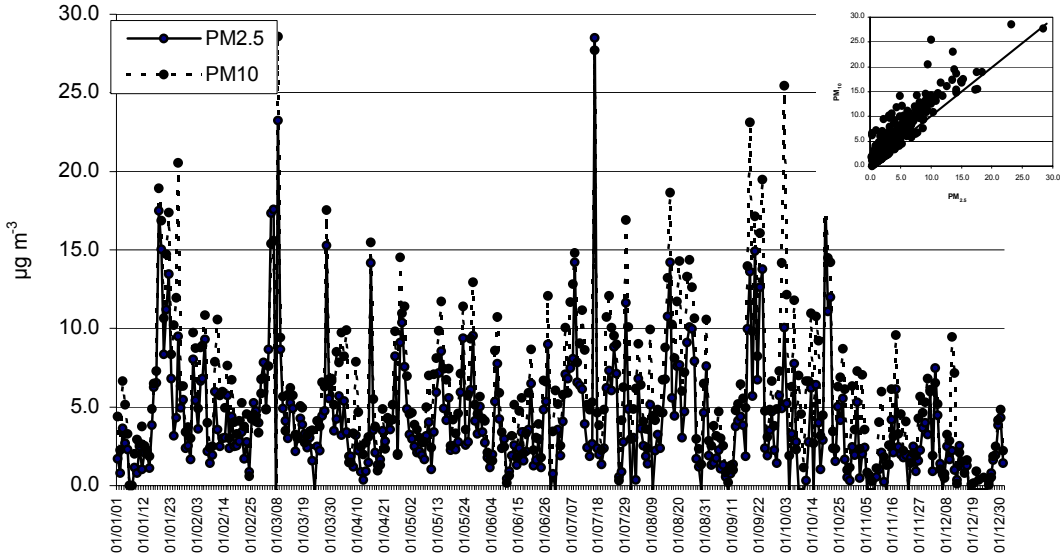

Figure 10: Time series and correlation between mass concentration of PM_{10} and $PM_{2.5}$ at Birkenes during the period of 1 Jan. 2001 - 31. Dec. 2001.

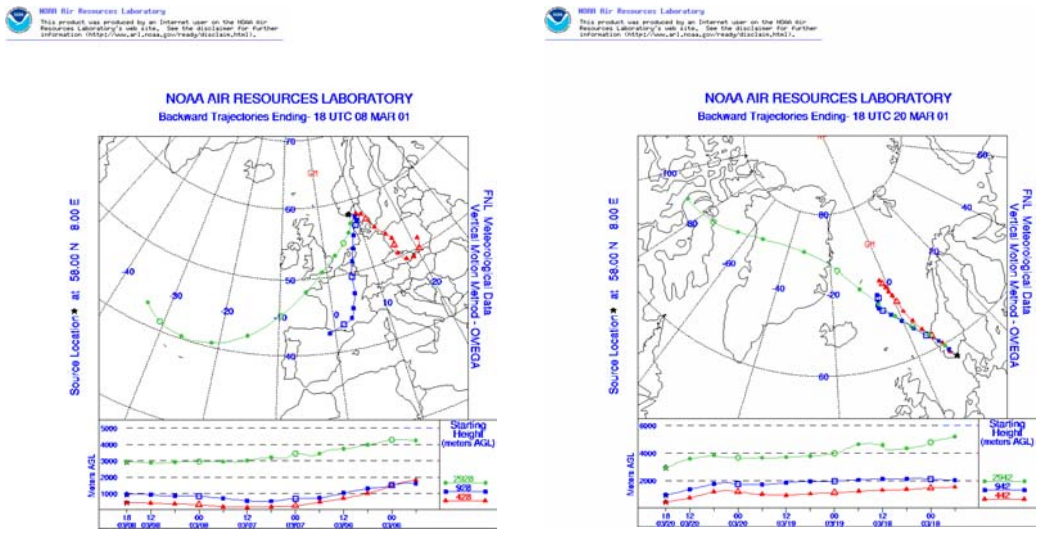

Figure 11: Air mass origin for two typical episodes representing high and low PM_{10} mass concentration respectively. Left: 8 March 2001; PM_{10}=28.6 µg m^{-3}, $PM_{2.5}$=23.2 µg m^{-3}. Right: 20 March 2001; PM_{10}=3.2 µg m^{-3}, $PM_{2.5}$=0.8 µg m^{-3} (HYSPLIT4 (HYbrid Single-Particle Lagrangian Integrated Trajectory) Model, 1997. Web address: http://www.arl.noaa.gov/ready/hysplit4.html, NOAA Air Resources Laboratory, Silver Spring, MD).

Table 3: Monthly-averaged mass concentration of the $PM_{2.5}$, $PM_{10-2.5}$ and PM_{10} fraction, and chemical components of the PM_{10} fraction during the period 01.01.01–31.12.01.

Month	$PM_{2.5}$	$PM_{10-2.5}$	PM_{10}	SO_4^{2-}	NO_3^-	NH_4^+	Cl^-, Na^+, Mg^{2+}	K^+, Ca^{2+}	OC	EC
January	4.65	2.12	6.80	1.62	0.53	0.35	0.53	0.05	0.61	0.15
February	3.96	1.58	5.54	1.08	0.31	0.15	1.09	0.05	0.86	0.18
March	5.97	0.69	6.66	2.01	0.89	0.66	0.64	0.08	0.63	0.11
April	3.96	1.93	5.89	1.35	0.53	0.32	0.61	0.05	1.81	0.20
May	4.08	1.80	5.89	1.14	0.35	0.27	0.27	0.06	2.29	0.15
June	2.78	1.46	4.24	1.44	0.44	0.44	0.42	0.07		
July	5.67	2.59	8.26	1.56	0.97	0.59	0.62	0.11		
August	4.96	2.92	7.88	1.86	0.62	0.57	0.55	0.08		
September	4.35	2.18	6.53	1.14	0.97	0.40	0.31	0.11	1.06	0.20
October	4.84	3.66	8.38	1.41	1.37	0.58	1.37	0.15	0.36	0.06
November	1.82	1.61	3.43	0.45	0.62	0.15	1.45	0.07	0.57	0.11
December	1.52	0.66	2.18	0.51	0.66	0.23	0.19	0.03		
Average	**4.05**	**1.93**	**5.97**	**1.30**	**0.69**	**0.39**	**0.67**	**0.08**	**1.02**	**0.15**

The sum of inorganic ions (here SO_4^{2-}, NO_3^-, NH_4^+, Ca^{2+}, K^+, Mg^{2+}, Na^+ and Cl^-) amounts on average to approximately 50-70% of PM_{10} based on monthly means (Figure 12, Figure 13, and Table 3), while the sum of SO_4^{2-}, NO_3^- and NH_4^+ contributes on the order of 30-50% to PM_{10}. The relative contribution of compounds of anthropogenic origin (SO_4^{2-}, NO_3^- and NH_4^+) to the PM_{10} mass concentration resembles the ratio of $PM_{2.5}$ to PM_{10}. Thus when $PM_{2.5}$ makes up a considerable part of PM_{10} the relative contribution from anthropogenic aerosols is most significant (Figure 12). Typically the constituents of marine origin (Na^+, Mg^{2+} and Cl^-) of the PM_{10} fraction amount to 10-25% on a monthly basis, and are highest during the winter season.

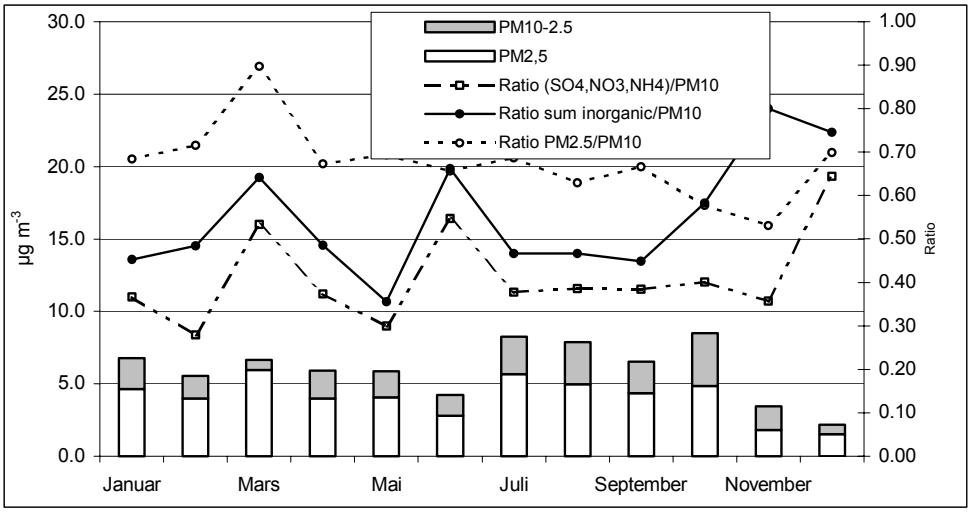

Figure 12: Monthly mean concentrations of PM_{10}, $PM_{10-2.5}$ and $PM_{2.5}$, ratio $PM_{2.5}$ to PM_{10}, ratio mass of inorganic compounds to PM_{10} and ratio of sulphate, nitrate and ammonium to PM_{10} at Birkenes.

The TC concentrations in the PM_{10} fraction range on a monthly basis from 0.4 to 2.4 µg C m^{-3} (Figure 14), making up 12–30 % of the PM_{10} mass concentration sampled by the LVS 3.1. The organic fraction typically accounts for 80–90% of the monthly averages of the TC concentrations during this period. The average monthly EC concentration is typically less than 0.2 µg C m^{-3} and contributes on average 2.0–3.6% of the PM_{10} mass concentration (LVS 3.1). Scatterplots of the EC and OC concentrations for both the $PM_{2.5}$- and the PM_{10}-fraction show a higher correlation for the $PM_{2.5}$-fraction, indicating contributions from different sources to the two fractions. During May and June an increase in OC is seen for both $PM_{2.5}$ and PM_{10}. However, the increase in the PM_{10} fraction is larger (see Figure 14). This might be due to coarse OC compounds of biogenic origin, which are highest in this season. A similar situation is encountered in October and may be explained by resuspension of biogenic material during autumn.

Due to technical problems no data are available during July–September 2001.

On a yearly average, the difference in concentration of OC, EC and TC in the PM_{10} fraction compared to the $PM_{2.5}$-fraction is very small. This clearly indicates that the majority of carbon containing particles lie in the size range below 2.5 µm, which is expected. However, comparing the monthly averages for February there seems to be an inconsistency as the $PM_{2.5}$ fraction has a higher concentration of OC and TC than the PM_{10} fraction. Although less pronounced, the same can be observed in April. The five samples collected in February all show considerably higher OC and TC concentrations (18–27%) for $PM_{2.5}$ than for PM_{10}. This indicates some kind of systematic error during sampling or during analysis.

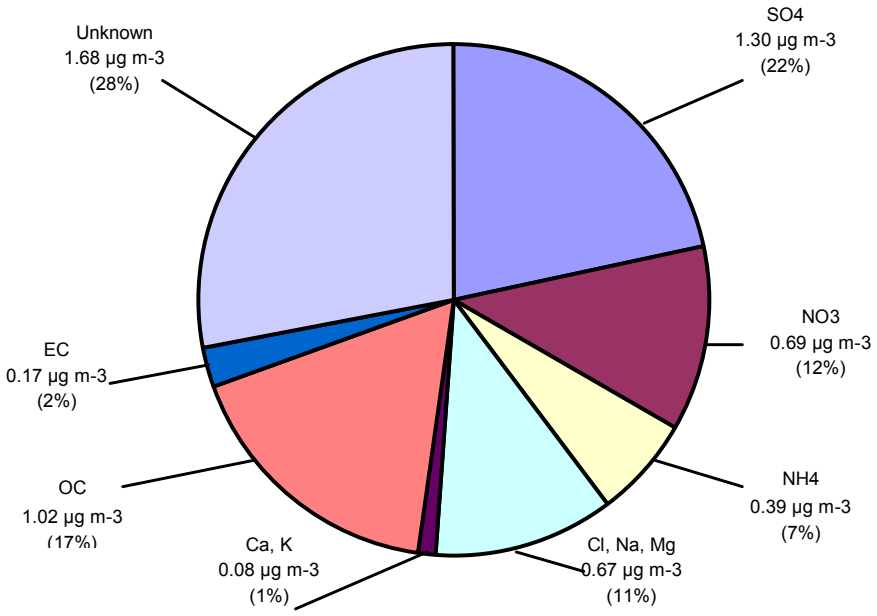

Figure 13: Mean chemical composition of PM_{10} at Birkenes 1.1.–31.12.2001 (average conc. = 6.0 µg m^{-3} (n = 363)).

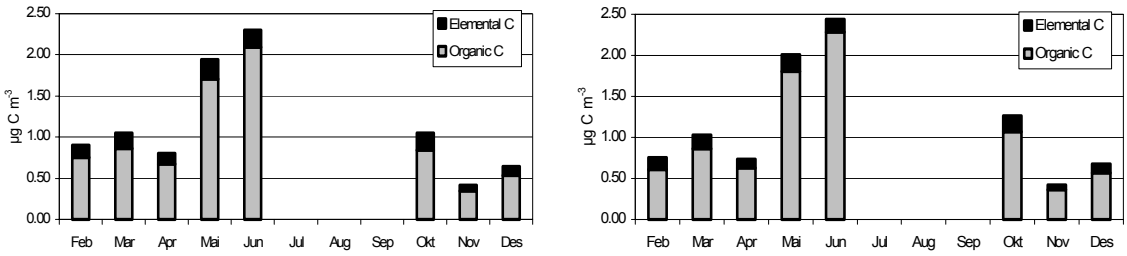

Figure 14: EC and OC concentrations for $PM_{2.5}$ (left) and PM_{10} (right). Results were only available for Feb.-Jun. and Oct.-Dec. 2001 (n = 30).

The carbonaceous content of $PM_{2.5}$ and PM_{10} was not analysed simultaneously, and a new set of sucrose standards was used during analysis of the $PM_{2.5}$ fraction. This may account for some of the observed differences. Use of a single quartz fibre filter to measure concentrations of carbonaceous particulate matter may lead to a considerable overestimation (known as "positive artefact") of the carbon content due to adsorption of organic vapours. The method based on using two filters in series proposed by McDow and Huntzicker (1990) and by Turpin et al. (1994) was devised to avoid this artefact. However the underlying theory is not straightforward and highly filter- and instrument-consuming. Preheating quartz fibre filters has been shown to generate a chemically highly active surface with an increased risk for adsorption of gases, which can cause a positive artefact. Nevertheless, quartz fibre filters in both LV samplers were preheated. Kirchstetter et al. (2001) demonstrated that there is a variation in the adsorption capacity of quartz fibre filters from different lots. If filters with a higher adsorption capacity have been used in the sampler that collected $PM_{2.5}$ during the first months of sampling, then a discrepancy may occur as the one we observed. However, no attempt has been made to estimate the possibility of positive artefacts due to adsorption of organic vapours in this study. Studies of sampling artefacts due to the use of quartz fibre filters are an important issue of concern, especially in remote areas.

Loss of mass may occur due to semi-volatile organic compounds (SVOCs) and ammonium nitrate evaporating from the filter after sampling. Transport, storage, and conditioning of filters are other important factors that may contribute to both negative and positive artefacts, and that must be considered along with other possible error sources associated with the sampling process. According to the filter pack data, the loss of nitrate by evaporation of nitric acid can be assumed to be less than 0.2 µg m^{-3} on average. Loss of Cl^- may also occur, but it is only important in episodes during which marine air masses dominate the sampling site. There have not been attempts to quantify positive or negative artefacts in this study.

The mass concentrations determined by the Partisol Dichotomous (Teflon filters) and the LVS 3.1 (pre-heated quartz filters) differ quite considerably, and neither the $PM_{2.5}$ nor the PM_{10} fractions are comparable within 5%. Comparing the 8-months-average of parallel sampling, the $PM_{2.5}$ and PM_{10} mass concentrations measured with the Dichotomous only amount to 83% and 78%, respectively, of the corresponding concentrations measured with the LVS 3.1. The largest

discrepancies occur during May and June, coinciding with the highest measured OC concentration. If also organic vapour concentrations are high at this time, adsorption onto quartz fibre filters may to some degree explain the observed discrepancy between the mass concentrations obtained with the two samplers. However, it should be noted that during periods of low anthropogenic influence the ambient concentrations are very low and in a range for which the determination of mass by weighing of filters is relatively uncertain.

A total of 72% of the mass concentration during the year can be identified by components quantified by ion- chromatography or evolved gas analysis. However, the parameters analysed in this study are not sufficient to give a complete mass closure. It is plausible that a significant part of the unknown fraction shown in Figure 13 is of mineral origin, and including this fraction into the monitoring programme would considerably reduce the percentage of unknown constituents. Using the most common components of the mineral elements obtained by ICP/MS analysis would reduce the unknown percentage further. Another part of the unknown fraction can most likely be attributed to the samples' water content.

The mass closure is a rough estimate and could be improved by multiplying the OC content by a factor between 1.2–1.9 to compensate for the relative amount of the elements O, H, S and N not being included in the EGA-analysis. A more detailed study is necessary to attain an extended knowledge of the relative percentages of the different constituents of the OC fraction. The water-soluble fraction of the OC should be multiplied by a factor at the higher end of the range. However, this fraction is known to vary considerably between different sampling sites. The mass closure uncertainty would be reduced if all chemical components could be obtained using the same filter. Using different samplers and different filter quality undoubtedly introduces a considerable degree of uncertainty.

5. Size resolved mass concentration and chemical composition of atmospheric aerosols over the eastern Mediterranean area

J. Smolik[1], V. Zdimal[1], M. Lazaridis[2], J. Schwarz[1], V. Havránek[3], K. Eleftheriadis[4], I. Colbeck[5], N. Mihalopoulos[6], S. Nyeki[5], C. Housiadas[4]

[1]Institute of Chemical Process Fundamentals, ASCR, Prague, Czech Republic
[2]Technical University of Crete, Department of Environmental Engineering, 73100 Chania, Greece
[3]Nuclear Physics Institute AS CR, Prague, Czech Republic
[4]N.C.S.R. Demokritos, 15310 Ag. Paraskevi, Attiki, Greece
[5]Department of Biological Sciences, University of Essex, UK
[6]Environmental Chemical Processes Laboratory (ECPL), Department of Chemistry, University of Crete 71409 Heraklion, Greece

5.1 Introduction

Two intensive measurement campaigns were performed at a remote coastal site on the Greek island of Crete and aboard the scientific boat "AEGAIEO" in the Eastern Mediterranean area between the Greek mainland and the island of Crete during 4 weeks in July 2000, and during 1 week in January 2001. The sampling site was the Finokalia station of the University of Crete. Finokalia (35^o 19´N, 25^o 40´E) is a remote coastal site east of Heraklion on the top of a hill (elevation 130 m) facing the sea within the sector from 270^o to 90^o. The site is shown in Figure 15 where back trajectories were performed on a daily basis to elucidate the origin of air masses arriving at the station. Depending on the weather, air masses reaching the station mainly originate from Europe and Africa.

The measurements aimed at assessing important components of the budget of airborne pollutants in the eastern Mediterranean area. These airborne pollutants are ozone, other oxidants, aerosols and precursors. These pollutants are derived mostly from emissions over the European continent, and are removed on time scales that allow them to be transported across national boundaries on the continent.

In addition to filter measurements, analysis of a large amount of data obtained from on-line instruments has been performed. On-line instruments include a Scanning Mobility Particle Sizer (SMPS), a laser aerosol spectrometer (LAS-X, Particle Measuring Systems), a three-wavelength integrating nephelometer (TSI model 3563), an Anderson Instrumentation aethalometer, and a number of gaseous analysers for O_3, NO_x, HONO, HNO_3.

In the current work we present and discuss results of the impactor sampling including collected particulate matter characterization. The filters obtained from the low pressure cascade impactor sampler (Berner low pressure impactor; BLPI) were complemented with subsequent chemical analysis by Ion Chromatography (IC) and PIXE analysis. In addition, analysis for elementary and organic carbon (EC/OC) was performed.

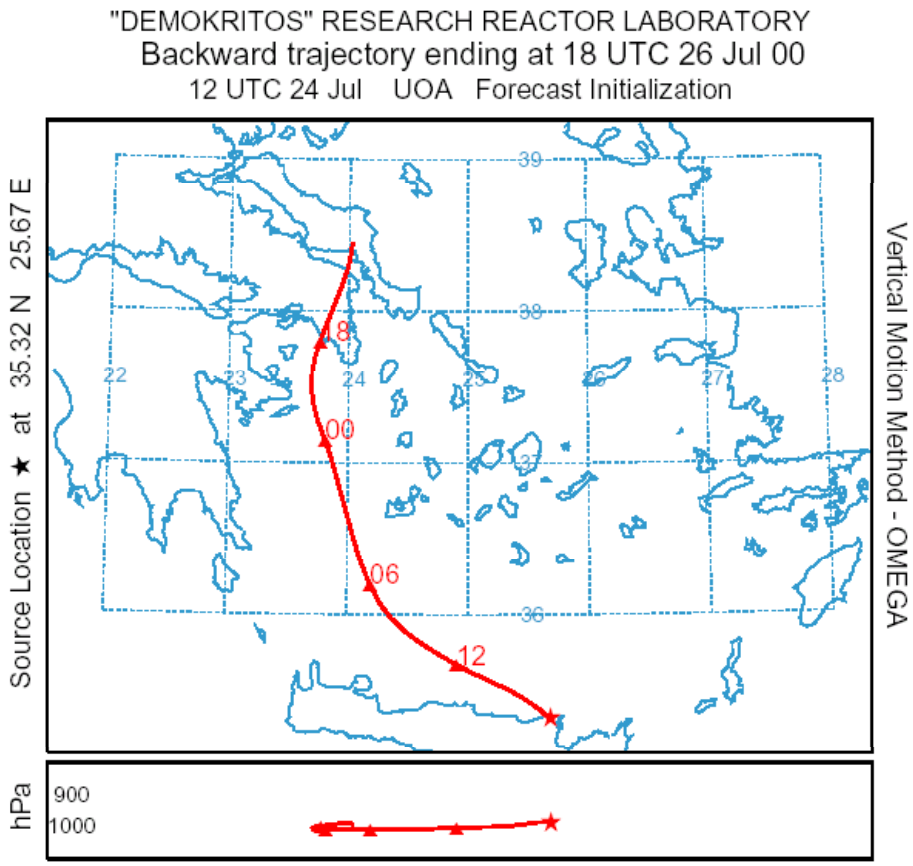

Figure 15: Back trajectory for the Finokalia station, Crete, Greece on 26 July 2000.

The impactor had an inlet with an upper particle size cut-off of approximately 15 µm (Liu and Piu, 1981) for a modified flow rate of 25 l/min. The samples were deposited on Nuclepore polycarbonate foils greased with Apiezon L vacuum grease. This reduced the particle bounce. Sampling was carried out in approximately 24-hour intervals.

In addition, atmospheric aerosol samples were also collected during the period 25–29 July 2000 aboard the research vessel "AEGAIEO". The vessel cruised the Aegean Sea along selected tracks calculated by forward and back trajectory modelling with the Finokalia sampling site as the end point.

Gravimetric analysis of aerosol samples

The mass distributions were determined from the weight difference before and after sampling due to deposited particulate matter on different foil stages. The electronic microbalances ATTA Cahn and Sartorius BP211D with a maximum attainable precision of 10 µg were used for weighing BLPI aerosol samples from the summer campaign and from the boat campaign, respectively. During the winter campaign Sartorius M5P-000V001 electronic microbalances with a maximum attainable precision of 1 µg were used. Foils were transported from the sampling site in Petri dishes and equilibrated in the weighing room for at least 24 hours before weighing. Internal calibration of the balance was performed

regularly, at least once at the beginning of each weighing run. To check reproducibility of the weighing procedure, a control aluminium foil was weighed at least once during each weighing run. Before and after each weighing run another control substrate (i.e. a blank made of the same polycarbonate foil and processed the same way, but without a sample) was weighed to check the influence of possible temperature and RH fluctuations.

Elemental analysis

All samples were analysed by particle-induced X-ray emission (PIXE). Analyses were performed with a 3MeV Van de Graaff electrostatic accelerator at the Nuclear Physics Institute in Řež at Prague. Two proton beam energies of 1.31 MeV and 2.35 MeV were used to irradiate samples. A 3 mm diameter collimator of the proton beam was chosen for stages 1 to 9. Stage 10 was analyzed with a 8mm collimator. Usually the proton fluence of about 10μC and 50μC were used for the 1.31 MeV and the 2.35 MeV measurement, respectively.

The typical time for one irradiation was about 5 min. The 1 mm polyethylene absorption filter was used for 2.35 MeV irradiation to reduce intensive low energy X-rays emitted from the sample. The PIXE-INP computer code (Havránek et al., 1994) was used to evaluate measured X-ray spectra. The following elements were measured during the summer Finokalia campaign and during the boat campaign: Al, Si, K, Ca, Ti, Mn, Fe, Sr, S, Cl, Ni, V, Cu, Cr, Zn, and Pb. During the winter campaign, a new set of polycarbonate foils with a low Br blank was used, which allowed determination of Br in aerosol samples. Elements up to Ti were determined with the 1.31 MeV beam, and the remaining elements were determined with the 2.35 MeV beam. The influence of observed matrix effects due to the deposit thickness was corrected by using the Equivalent Layer Thickness Model (Havránek et al., 1999). In this case we used the function of the Fe signal depression ratio on the deposit mass for particulate impactor stages to estimate the effective deposit thickness.

5.2 Mass size distributions

A total of 21 mass size distributions from the summer campaign, 5 from the boat campaign, and 7 from the winter measurements were obtained. The distributions were predominantly bimodal with mode mean diameters around 0.4 and 5 μm and with a minimum between both modes at around 1 μm. Such distributions seem to be typical for atmospheric aerosols collected by different impactors at different locations (see e.g. Horvath et al., 1996). However, the low pressure impactors are not sensitive enough (due to the low mass concentration of atmospheric particles < 100 nm, typically sampled volume, accuracy of weighing, and number of collection stages in this range) to determine mass size distributions in the Aitken nuclei range (Horvath et al., 1996, Mäkelä et al., 2000).

The raw mass size data were inverted into smooth mass size distributions by the MICRON code (Wolfenbarger and Seinfeld, 1990). The inverted distributions were integrated to obtain PM_1 and PM_{10}. The time series of PM_1 and PM_{10} for both summer (Finokalia station and boat) and winter campaigns are shown in Figure 16–Figure 18. In Figure 16, three different periods can be identified. During the first period (10–17 July 2000) the PM_{10} mass concentration varied between 20 to 40 $\mu g/m^3$. During the next period (18–25 July 2000) the PM_{10} mass

concentration was practically constant around 30 μg/m^3. After 25 July it increased within two days up to almost 70 μg/m^3 (27th July 2000) followed by a drop to about 35 μg/m^3 (30 July 2000). The PM_1 concentrations increased gradually during the whole period from about 5 to about 15 μg/m^3.

The wind conditions, measured at Finokalia station, were nearly constant during the summer measurements, except during the last three days. The wind direction was NW (300-320°), and the wind velocity was 8-12 m/s. During the three last days the wind direction varied between 110-360° with a wind velocity around 1m/s. Since the local wind conditions cannot explain the observed temporal variation of PM_1 and PM_{10}, backward trajectories ending at Finokalia station (35,32 N, 25.67 E) were computed with 6-hour time steps using HYSPLIT4 Trajectory Model (NOAA Air Resources Laboratory, 2001). The trajectory computations started 72 hours back in time before 10. July 2000 at 10:00 (local time). The results show that during the first period (10–17 July 2000) air mass back trajectories arriving in Crete originated between the north and the west.

At the beginning of the campaign air masses first came from the west, but they later recirculated over eastern Greece and Turkey reaching Finokalia from the north. On the fourth day of sampling air masses originated above Northern Africa, arriving at Finokalia from the west. During the next four days, air masses came again from Western Europe with a peak velocity on the 7th day of sampling. In the following period (18–28 July 2000) the air masses reached Finokalia from the north. They originated mainly from the western coast of the Black Sea, except during the last three days of this period, when peak mass concentrations were observed, and when the air masses originated from the Aegean Sea. On the last two days, trajectories originated north of Crete, moved first to Africa and then changed direction, finally arriving at the Finokalia site from the southeast.

In Figure 17, mass concentrations of PM_1 and PM_{10} from the boat measurements are shown. Due to some technical problems samples on the boat were not taken at standard times as at the Finokalia station, hence sampling times were usually shorter. Although the boat tried to follow computed backward trajectories, local changes in the wind direction occasionally occurred during sampling. At the end of the boat campaign there were several days with almost calm air. The direct comparison of both sets of data using backward wind trajectories and position of the boat with respect to Finokalia station is difficult. Nevertheless, the boat data show similar trends in PM_{10} concentrations as those obtained at Finokalia. It can also be seen that both PM_1 and PM_{10} concentrations were higher on the boat as compared to Finokalia station.

Figure 18 shows PM_1 and PM_{10} mass concentrations measured at Finokalia station during the winter campaign. In comparison with summer measurements both PM_1 and PM_{10} were lower. PM_1 decreased during the whole period from 9 to 4 μg/m^3 with a minimum of almost 2 μg/m^3 during the middle of the campaign, whereas PM_{10} varied between 10 and 20 μg/m^3. The temporal variations of PM_1 and PM_{10} were rather smooth in comparison with the summer data. Winter samples were collected from air masses coming from different directions.

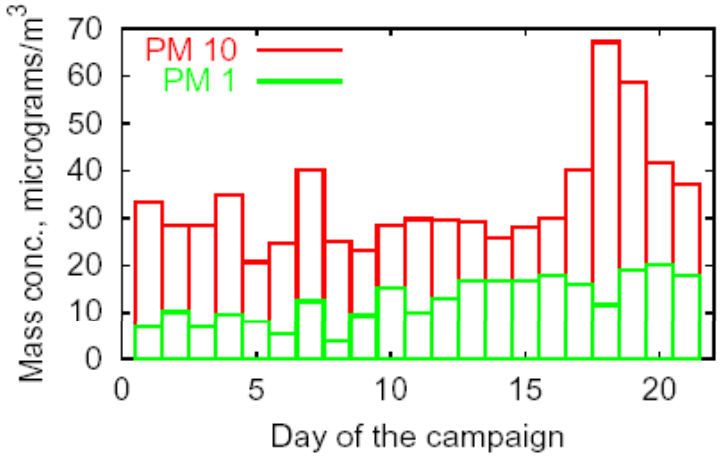

Figure 16: Daily PM_1 and PM_{10} mass concentrations at Finokalia 10–31 July 2000.

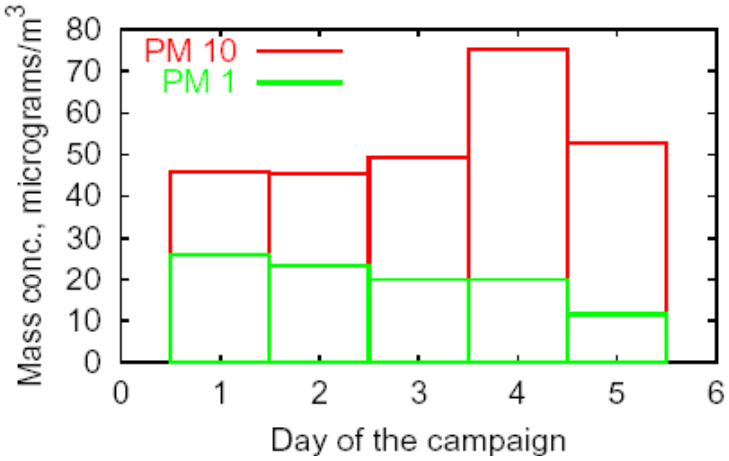

Figure 17: Daily PM_1 and PM_{10} mass concentrations aboard of the research vessel "AEGAIEO" 25–29 July 2000.

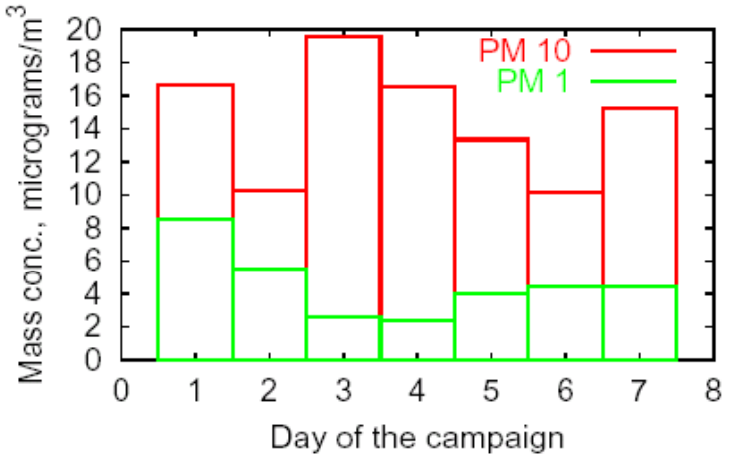

Figure 18: Daily PM_1 and PM_{10} mass concentrations at Finokalia 17-24 January 2001.

On the first day of winter sampling the HYSPLIT4 Trajectory Model computed air mass trajectories originating north of Greece, recirculating south of Crete, and arriving from the south at the station. On the next day, southerly winds dominated, and air masses arrived from Africa. During the next four days the air masses reached Finokalia from the northwest.

With decreasing wind velocity, air masses originated first above the Atlantic Ocean and later above Western Europe, the Ligurian Sea, and finally above southern Italy. On the last day southerly winds dominated with air masses coming first from the Mediterranean Sea and later from Africa. Summarising the results from the summer and winter campaigns at Finokalia the lowest mass concentrations of PM_1 and PM_{10} were observed for air masses arriving with low wind velocity from the Mediterranean Sea. Higher mass concentrations were observed for air masses arriving from the Atlantic Ocean and from Western Europe, Northern Africa or across the northern coast of Turkey.

5.3 Elemental size distributions

As already mentioned in previous paragraphs Al, Si, K, Ca, Ti, Mn, Fe, Sr, S, Cl, Ni, V, Cu, Cr, Zn, and Pb were determined in the BLPI samples using PIXE analysis. In addition a new set of polycarbonate foils with low blank values of Br was used during the winter campaign that allowed to determine also this element in aerosol samples. Typically samples collected on stages 1-6 (i.e with particles < 1 μm in diameter) were black, thus indicating the presence of soot from combustion. The samples with coarse particles were beige in colour, corresponding to mineral dust. Principally three types of elemental size distributions were observed.

A monomodal distribution with a mode centred at about 4 μm was typical for the crustal elements Al, Si, Ca, Ti, Mn, Fe, and Sr, although multimodal distributions were also observed for Al, Si, Ti, and Mn in some samples collected during the winter campaign. Cl also exhibited a monomodal distribution with a maximum around 5 μm. Bimodal distributions with modes at around 0.3 and 3 μm were observed for S, Br, K, V, and Ni. The fine mode was dominant for S in all samples and for Ni and V in those samples collected on the boat.

Anthropogenic elements Cu, Cr, Zn, and Pb showed rather flat multimodal distributions that were centred at about 1 μm. Such types of elemental size distribution also seem to be typical for atmospheric aerosols collected by different impactors at different locations (see e. g. Horvath et al., 1996). The coarse mode of crustal elements corresponds to mineral dust. The submicrometer mode, observed during winter, is an indication for anthropogenic origins (probably fly ash from coal combustion). Chlorine in the coarse mode shows sea-salt particles produced by bursting of bubbles. The size distribution of sulphur in aerosols is dominated by the accumulation mode. This shows that sulphur-containing compounds in aerosols are mainly a product of gas-to-particle conversion (Finlayson-Pitts and Pitts, 2000).

Bimodal distributions of K, Ni, and V in aerosol particles indicate that these elements are of both anthropogenic and natural origin. Potassium in submicrometer particles results from biomass burning, while nickel and vanadium come from oil combustion. Rather broad distributions of Cu, Cr, Zn and Pb with not too

well-defined peaks indicate multiple sources and aged aerosol. Occasional fine and coarse mode peaks in Cu illustrate that this element can be attributed to anthropogenic and crustal sources.

The raw elemental size data were inverted into smooth elemental size distributions using the MICRON code, and the inverted distributions were integrated to obtain PM_1 and PM_{10}. The time series of PM_1 and PM_{10} for both the summer (Finokalia station and boat) and the winter campaigns are shown in Figure 19–Figure 21.

From Figure 19a two peaks in the concentration of crustal elements Al, Ca, Fe, K, Mn, Si, Sr, and Ti can be seen, one appearing at the beginning and the other one at the end of the summer Finokalia campaign. Moreover, these peaks have a very similar shape for all these elements, indicating the same source during both periods. As found from the backward trajectory, calculated for the fourth day of measurements, the source could be Saharan dust. The same source can be expected for the peak concentrations observed at the end of the summer campaign.

Relatively high concentrations of potassium in PM_1 indicate biomass burning as a source. Higher concentrations observed at the beginning of the campaign can be attributed to forest fires

The time series for sulphur, chlorine, and some trace elements are shown in Figure 19b. As can be seen sulphur was found mainly in the fine particle mode. Lower concentrations were observed for conditions where air masses originated from Italy, the Ligurian Sea, and the Mediterranean Sea west of Crete (5th-8th day of measurements). Higher concentrations were observed for air masses arriving from the west coast of the Black Sea (9th-19th day of measurements). The opposite behaviour was found for chlorine, for which high concentrations were observed for air masses coming from the west (usually with higher wind velocity) and very low concentrations were found for air masses from the north, originating near the west coast of the Black and Aegean Seas and arriving with low wind velocity. These observations may be related to the wind velocity, since the number of sea-salt particles is approximately exponentially related to wind speed (Pósfai and Molnár, 2000).

The trace elements Cr, Cu, Ni, Pb, V, and Zn were found in both the fine and the coarse particle modes, indicating both anthropogenic and natural origins. In principle, the time series of both PM_1 and PM_{10} for Cu, Pb, and Zn resemble the behaviour of sulphur. In Figure 20a,b results from the boat measurements are shown. As in the Finokalia observations the crustal elements Al, Ca, Fe, K, Mn, Si, Sr, and Ti were predominantly found in the coarse mode, and they exhibit a similar behaviour. This shows again that these elements are mainly soil derived. The concentrations of these elements are comparable with concentrations found during corresponding days at Finokalia station, thus indicating a similar origin. Cr behaved identically to the crustal elements. Concentrations of Cl, found again only in the coarse mode, were also higher than those observed at Finokalia. Concentrations of V and Ni measured on the boat were higher than those at Finokalia. This can be attributed to the additional emissions from the oil driven

engines of both the "AEGAIEO" and other vessels cruising in the area of measurements. Sulphur was found in both the fine and coarse modes with concentrations comparable to those observed at Finokalia. It is worth noting that the time series for Cu, Pb, and Zn are very similar to that of sulphur.

Results from the winter campaign are shown in Figure 21a,b. Again the crustal elements exhibit a similar behaviour, although the agreement is not as good as found during the summer campaign. This may be due to the higher concentrations of Al and Si found in the PM_1 fraction as compared to the corresponding concentrations observed during summer. This can be attributed to higher emissions from combustion processes in winter (Ondov et al., 1981; Horvath et al., 1996). The high concentration of K indicates combustion of biomass as a source. Sulphur was found both in fine and coarse modes, chlorine practically only in the coarse mode. Time series for V and Ni are similar, with high contributions of fine particles. This again points to oil combustion as a likely source. Cu and Zn exhibit trends similar to S. The mass spectrum of Cr is broad with no well-defined distribution.

The time series of crustal and trace element concentrations in PM_1 and PM_{10} reflect different air masses arriving at Finokalia during the winter sampling period. Air masses first came from the south of Greece and later recirculated over the Mediterranean Sea and Northern Africa. After that air masses arrived from the Atlantic Ocean over Northern Africa and later over Western Europe. Finally, on the last day of measurements air masses again originated over the Mediterranean Sea and recirculated over Northern Africa. The air masses coming from Africa correspond to high concentrations of crustal elements observed on the 3rd and 7th day of measurements. The natural origin of the particles is also corroborated by a very low contribution of crustal elements to the PM_1 fraction observed on these two days. Quite like in the results obtained during the summer campaign, high concentrations of Cl were observed in air masses coming from the Atlantic Ocean. The Cl concentrations decreased with decreasing wind velocity. The highest concentration of sulphur was found for an air mass advected from Southern Greece.

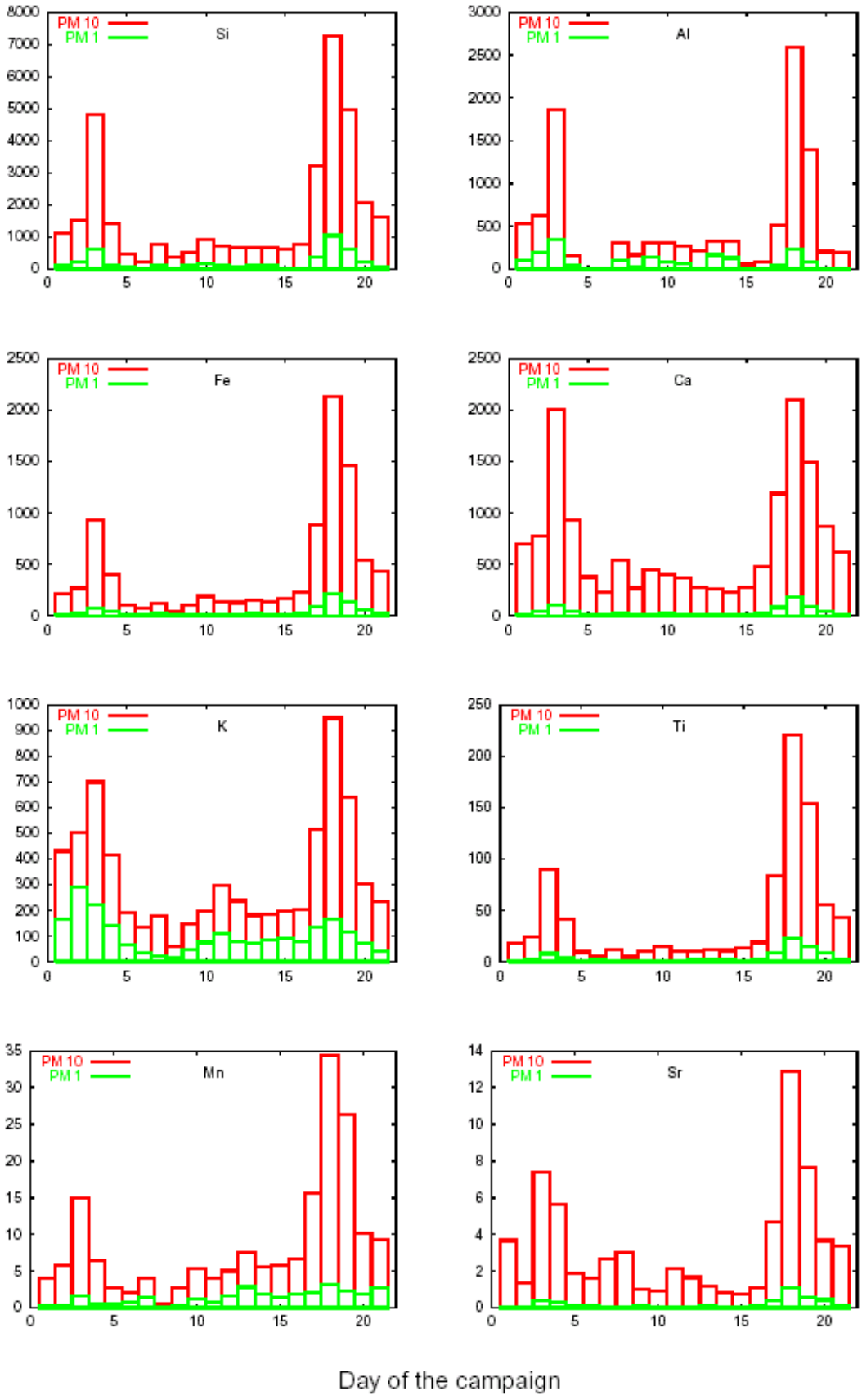

Figure 19a: Daily crustal element concentrations in PM_1 and PM_{10} at Finokalia 10- 31 July 2000 (units: ng/m^3).

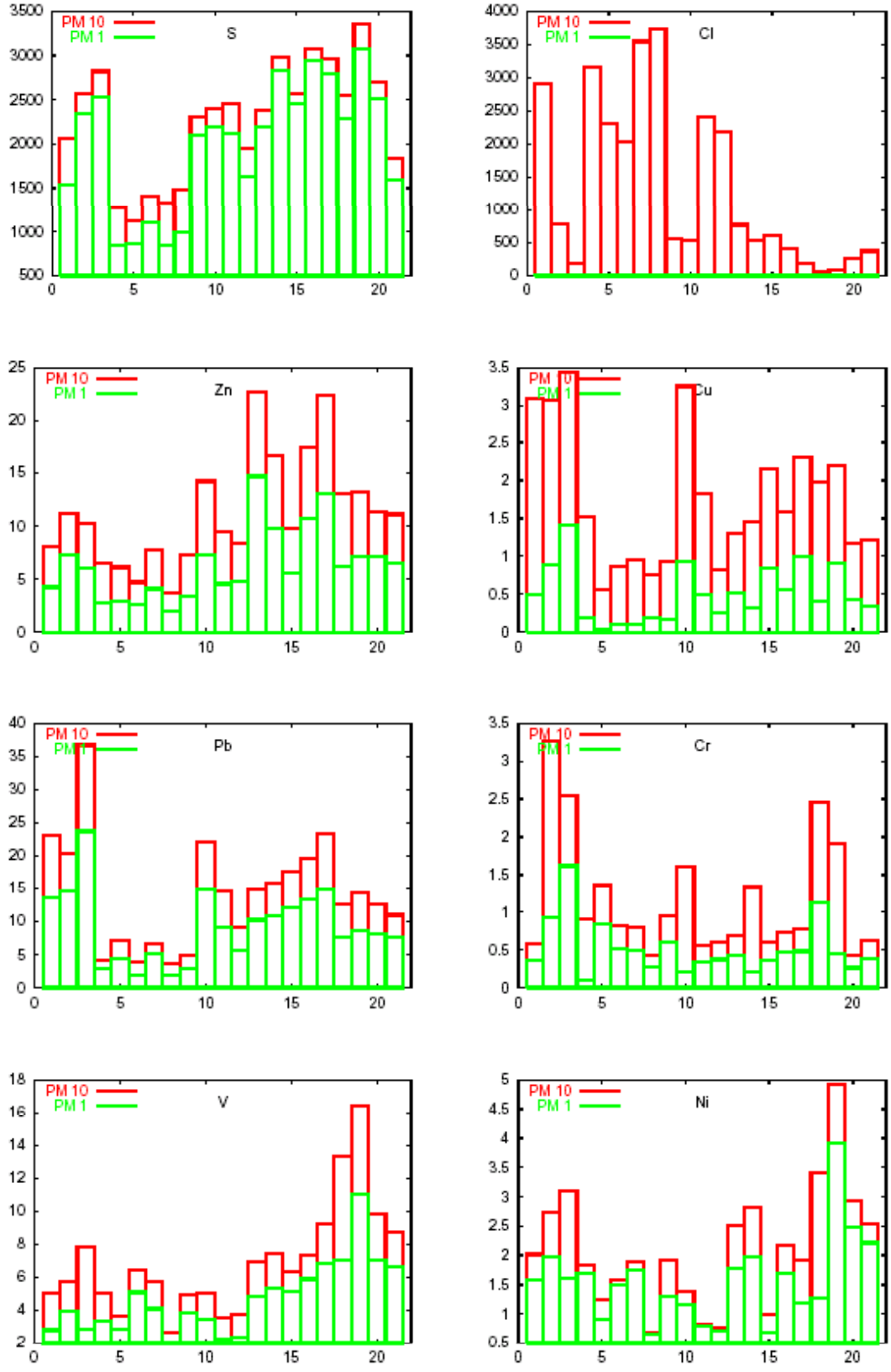

Figure 19b: Daily sulphur, chlorine, and trace element concentrations in PM_1 and PM_{10} at Finokalia 10–31 July 2000 (units: ng/m^3).

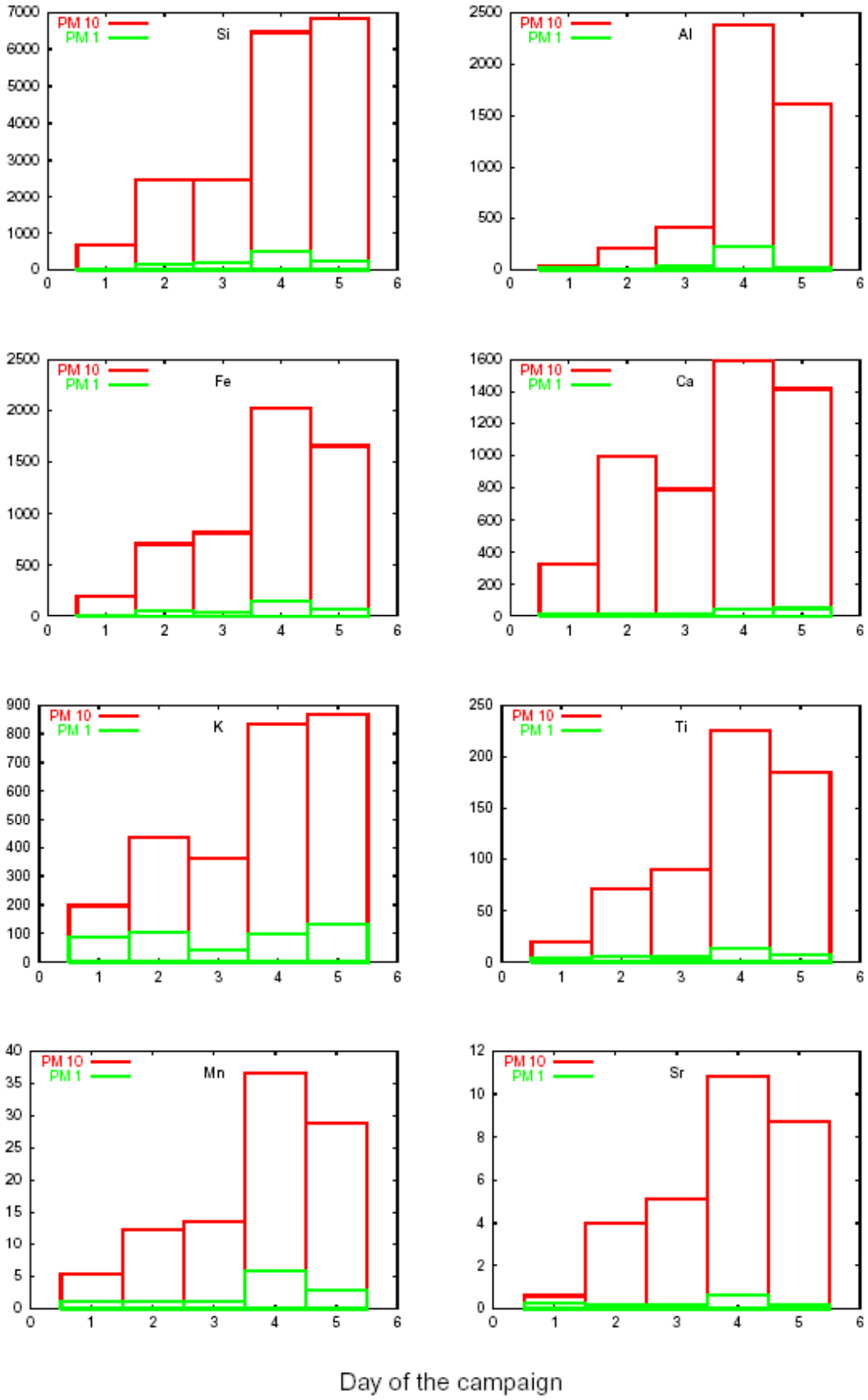

Figure 20a: Daily crustal element concentrations in PM_1 and PM_{10} aboard the research vessel "AEGAIEO" 25–29 July 2000 (units: ng/m^3).

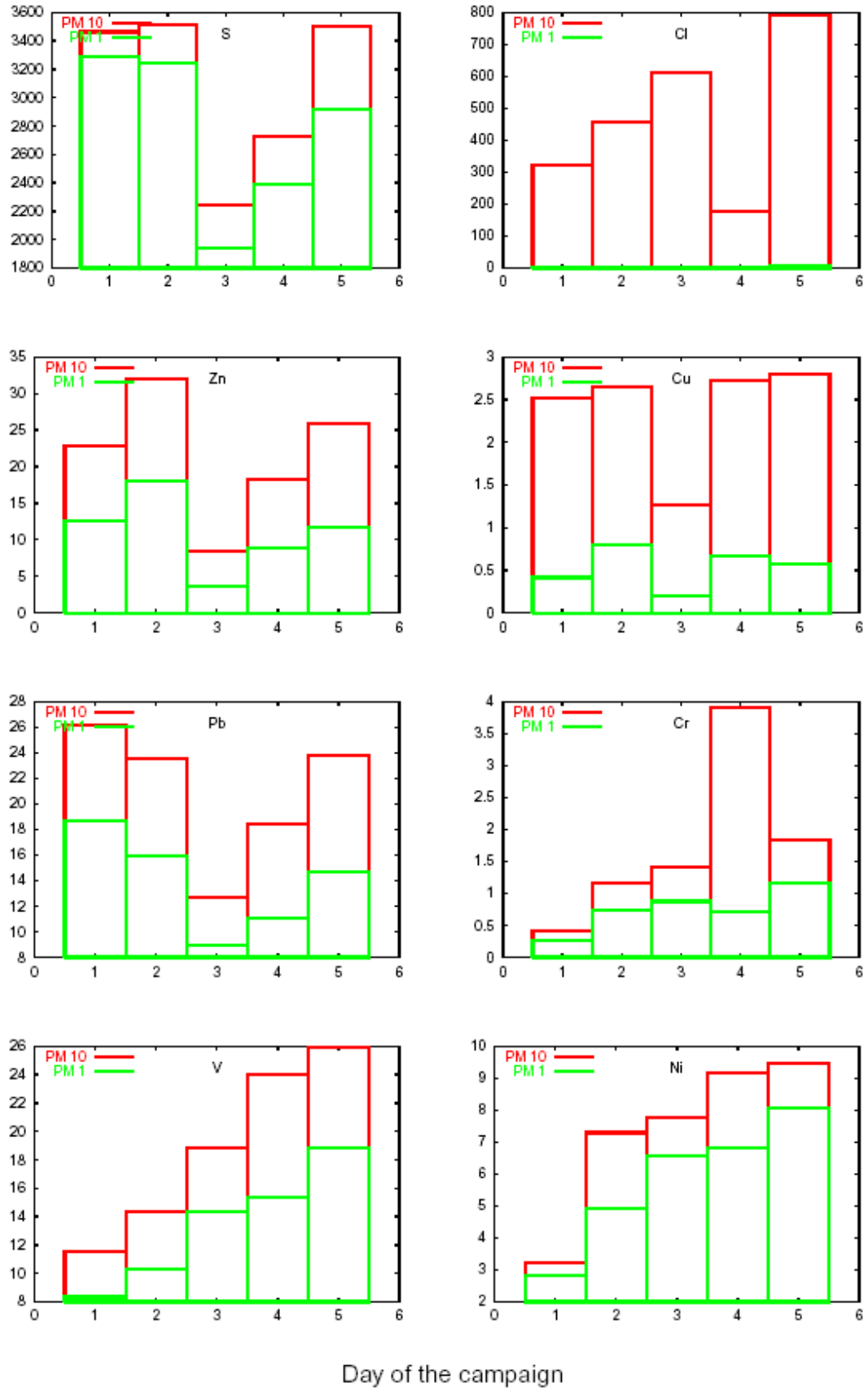

Figure 20b: Daily sulphur, chlorine, and trace element concentrations in PM_1 and PM_{10} aboard the research vessel "AEGAIEO" 25–29 July 2000 (units: ng/m^3).

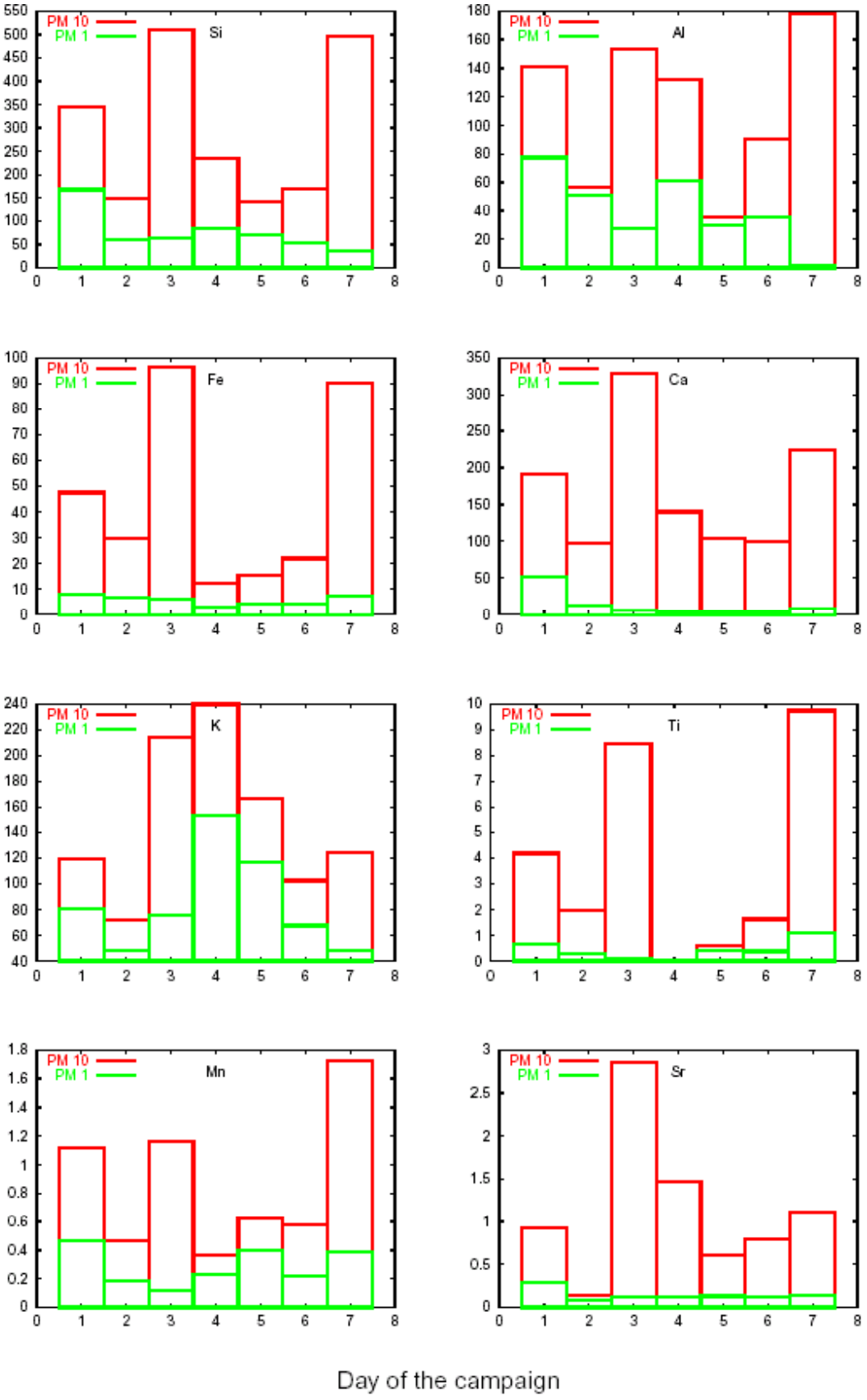

Figure 21a: Daily crustal element concentrations in PM_1 and PM_{10} at Finokalia 7–14 January 2001 (units: ng/m^3).

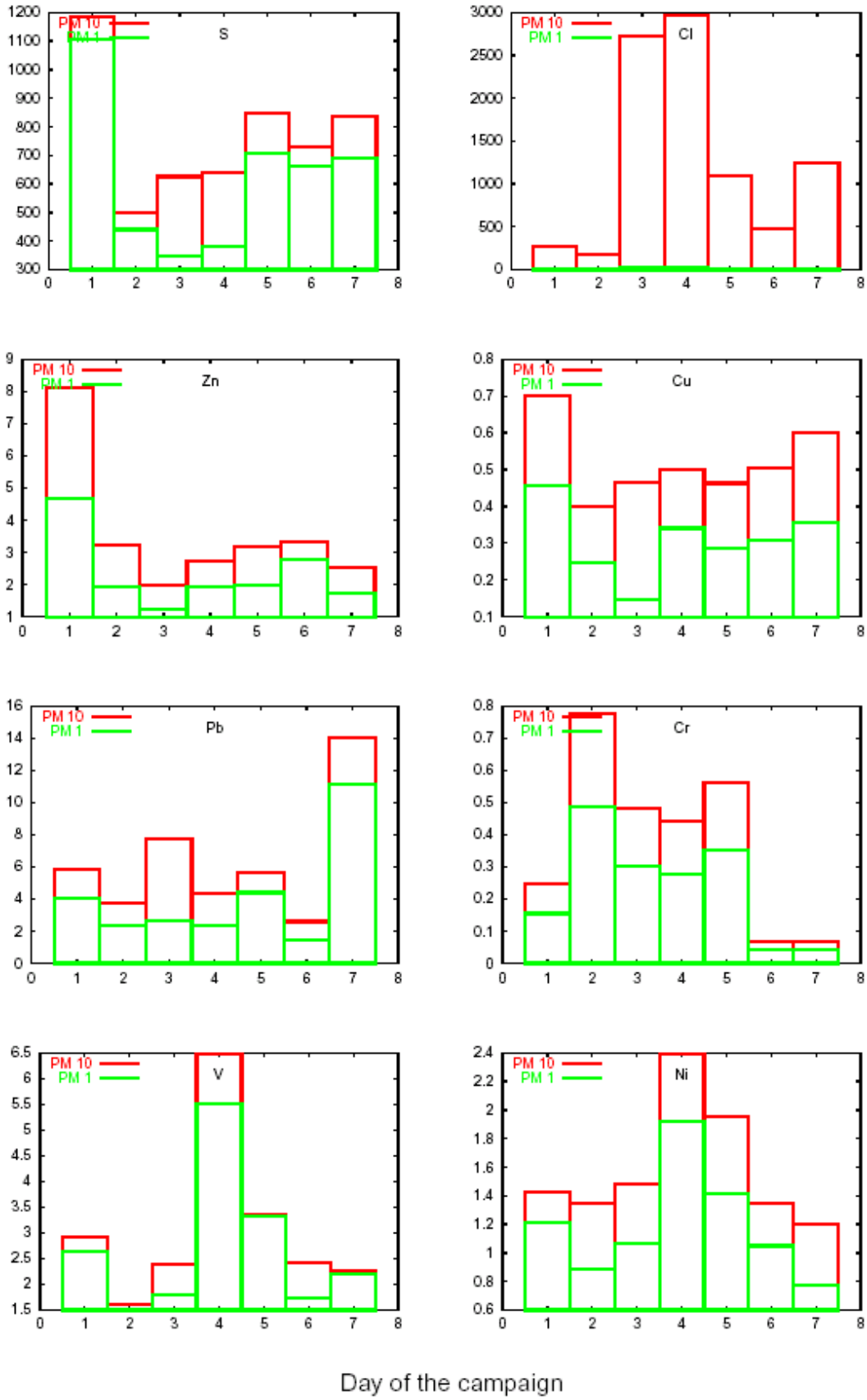

Figure 21b: Daily sulphur, chlorine, and trace element concentrations in PM_1 and PM_{10} at Finokalia 7–14 January 2001 (units: ng/m^3).

5.4 Chemical size distributions

All impactor samples were analysed by ion chromatography for SO_4^{2-}, NO_3^-, Cl^-, K^+, Na^+, NH_4^+, Ca^{2+}, and Mg^{2+} (except samples from the 3rd day of the summer campaign at Finokalia and from the last day of the boat campaign). Sulphate and ammonia were predominantly found in fine particles, whereas nitrate, chloride, sodium, calcium, and magnesium were mostly found in coarse particles. Potassium was mainly found in the coarse fraction, but several samples also exhibited bimodal distributions. As in previous cases the raw ion size data were inverted into the ion size distributions using the MICRON code, and the inverted distributions were integrated to obtain PM_1 and PM_{10}.

Figure 22 shows time series of PM_1 and PM_{10} for individual ions from the summer campaign at Finokalia. As can be seen the time series of Cl^-, Na^+, and Mg^{2+} are similar. The average atomic ratio Mg^{2+}/Na^+ during the first two weeks was 0,125, which is very close to the value of 0,121 obtained for typical seawater composition (Finlayson-Pitts and Pitts, 2000). It shows that both elements originate from seawater droplets. During the last days this ratio increased up to 0,37.

A higher content of Mg may come from Saharan dust that contains dolomite (Schütz and Rahn, 1982). Further, a chloride anion deficiency was observed relative to sodium concentrations with an atomic ratio Cl/Na varying in the range 0.4 - 1. This may result from the reaction of solid sea salt particles with gaseous acids or NO_2 that produces solid sodium nitrate (Finlayson-Pitts and Pitts, 2000). This would also explain the presence of nitrate in coarse particles. Ammonia and sulfate that were found in the fine particle mode indicate the presence of ammonium sulfate and bisulfate. Plotting the sulphate concentration versus the ammonia concentration it was found that both ammonium sulphate and bisulphate were collected during the summer campaign except in the last week of measurements, when high concentrations of ammonia were observed. High concentrations of ammonia were also found in samples from the boat, collected practically at the same time.

The boat results are shown in Figure 23. Cl^-, Na^+, and Mg^{2+} exhibit a similar behaviour. Here the atomic ratio Mg^{2+}/Na^+ varied between 0.17 and 0.33. As the sampling on the boat was carried out at the same time when relative high concentrations of Mg^{2+} were observed at Finokalia we can conclude that the same source was responsible for the high concentrations of Mg^{2+}. Further, we observed a substantial chloride ion deficiency in these samples relative to sodium with an atomic ratio Cl^-/Na^+ lying between 0.35–0.47. Figure 24 shows results from the winter campaign. The time series for Cl^-, Na^+, and Mg^{2+} show again similar trends.

The atomic ratios Cl^-/Na^+ and Mg^{2+}/Na^+ varied between 0.85-1.25 and 0.125-0.36, respectively. The values that were closer to the typical seawater composition were observed on days when air masses came from the Atlantic Ocean after crossing western Europe. In addition, the ammonia/sulphate ratio corresponded only to ammonium sulphate. Finally, for all samples collected during the summer and winter we compared concentrations of chloride and nitrate anions with concentrations of sodium and magnesium cations in PM_{10}. It was found that these ions are practically counterbalanced.

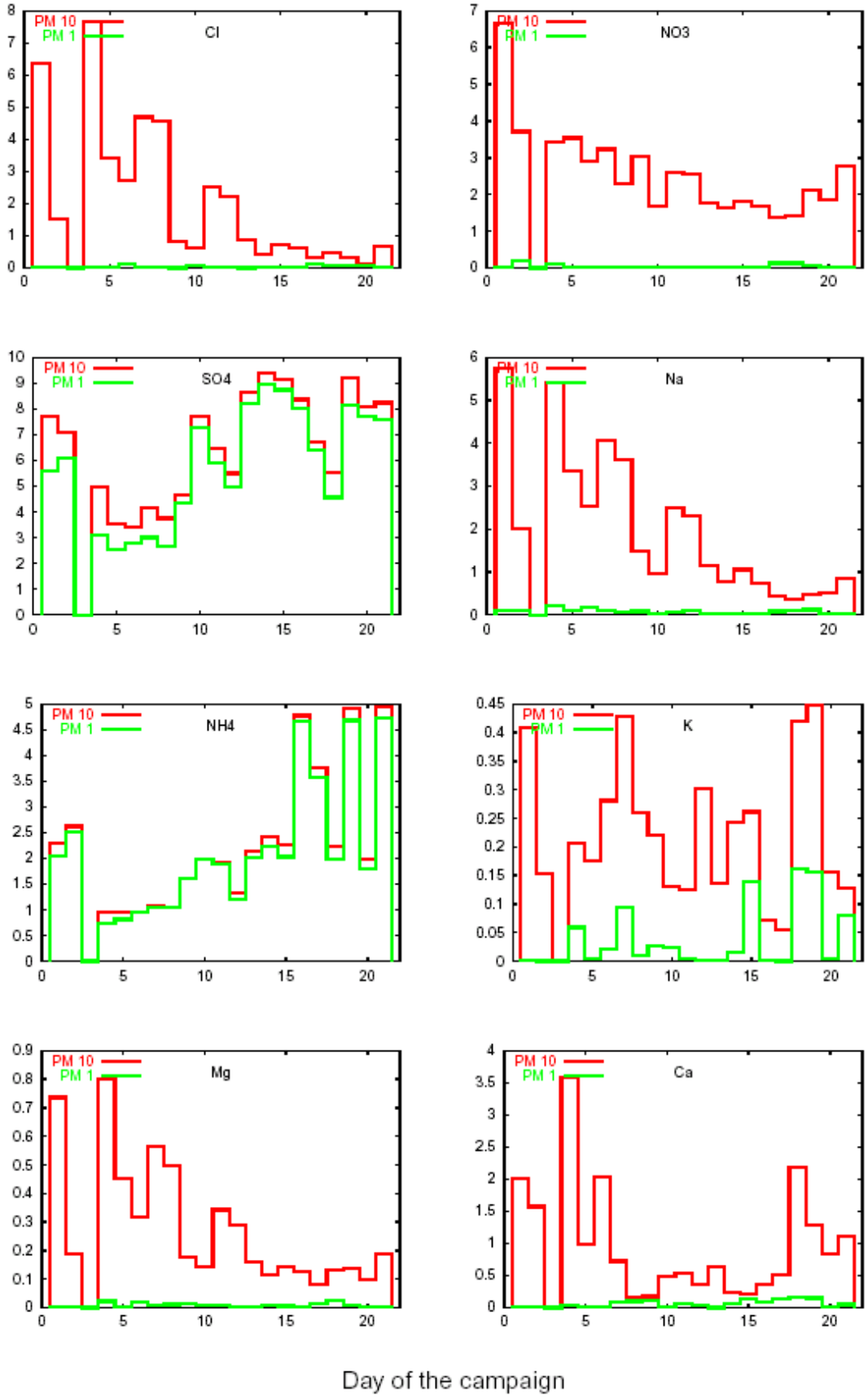

Figure 22: Daily ion concentrations in PM_1 and PM_{10} at Finokalia 10–31 July 2000 (units: µg/m^3).

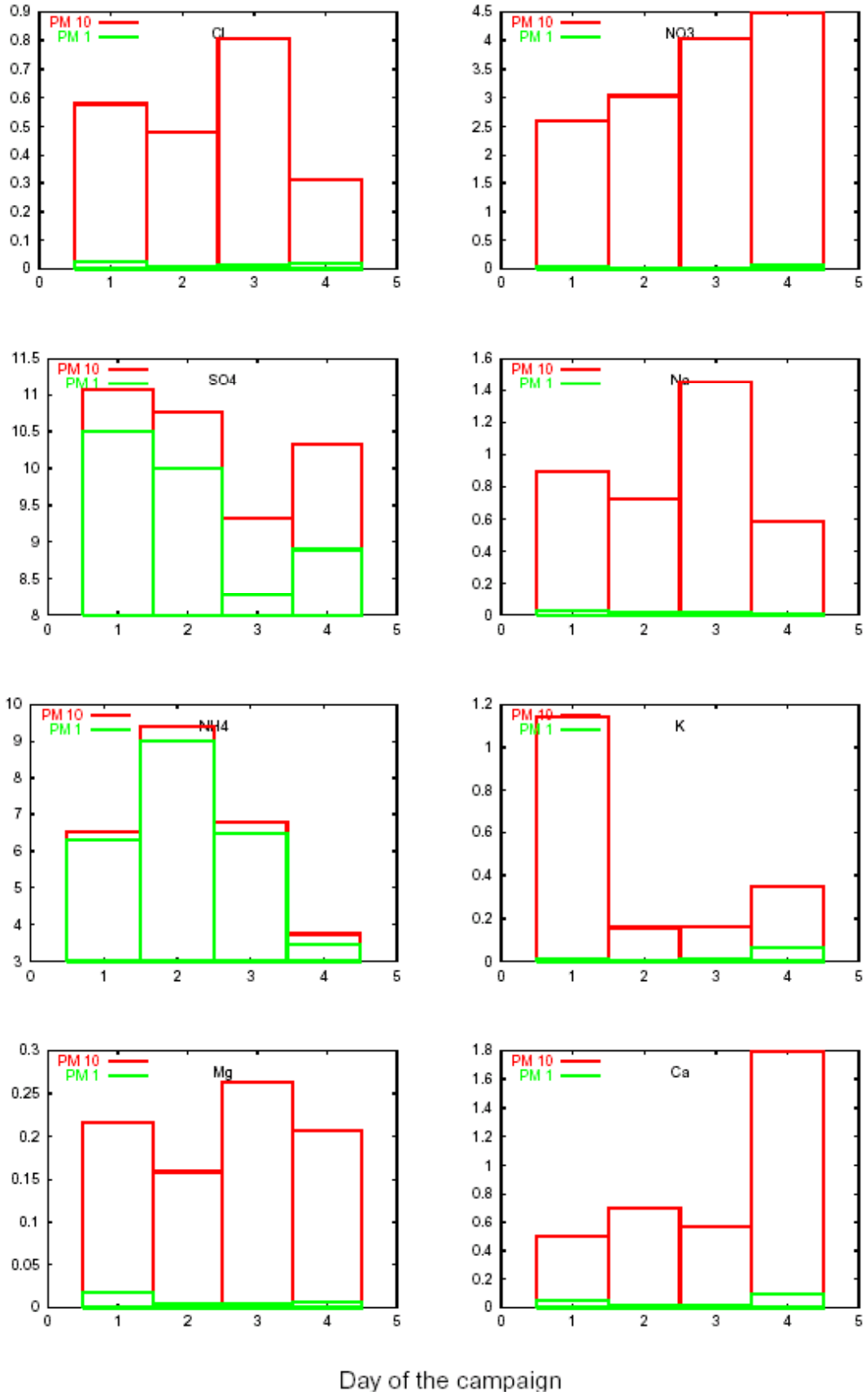

Figure 23: Daily ion concentrations in PM_1 and PM_{10} aboard the research vessel "AEGAIEO" 25–29 July 2000 (units: µg/m^3).

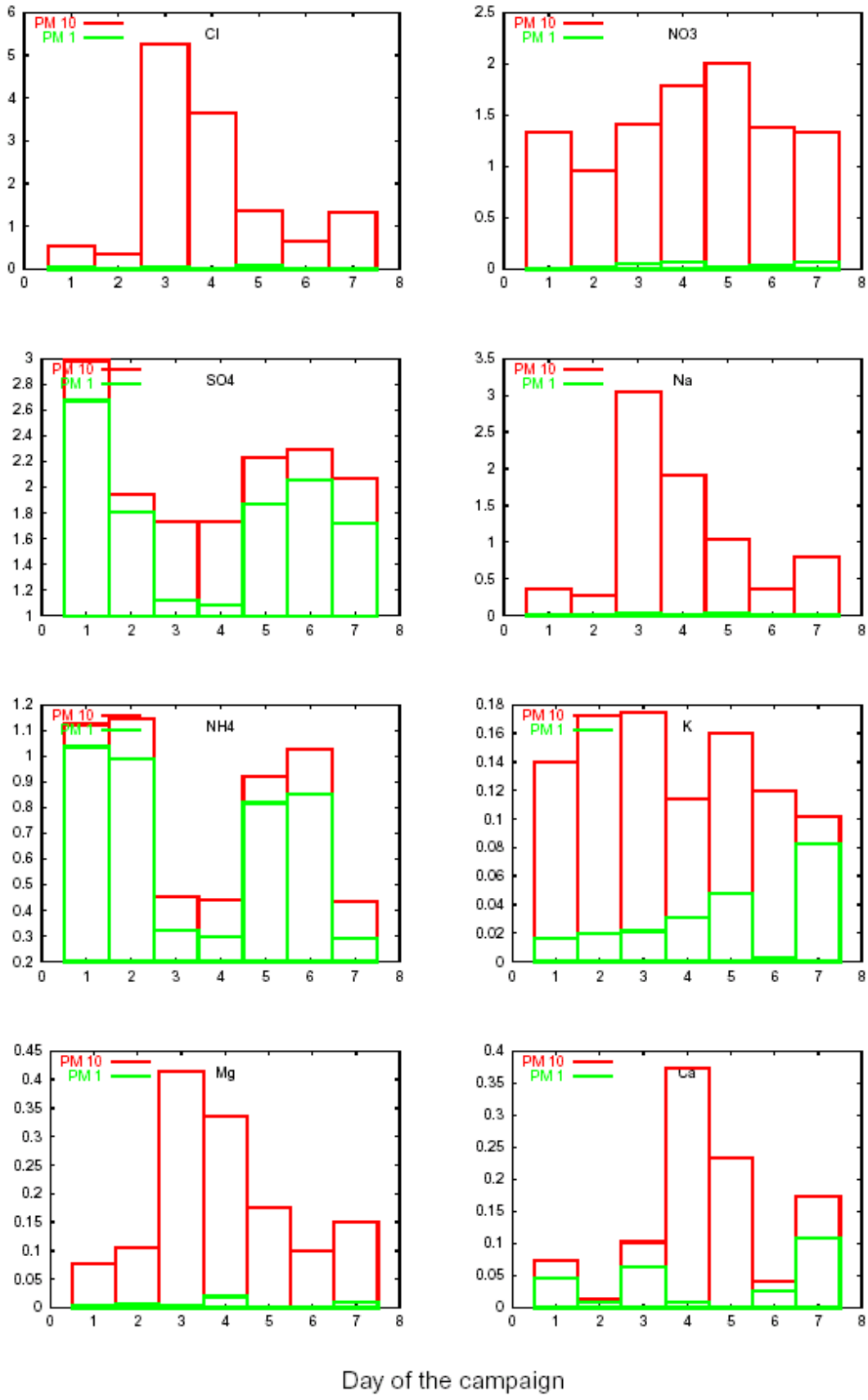

Figure 24: Daily ion concentrations in PM_1 and PM_{10} at Finokalia 7–14 January 2001 (units: µg/m^3).

5.5 Organic mass

In addition analysis of both elemental (EC) and organic carbon (OC) collected with eight filters during summer and eight filters during winter was performed using a thermo-optical determination technique. Although concentrations varied between 0.09-0.68 μg m^{-3} and 0.28-2.23 μg m^{-3} for EC and OC, respectively, their ratio (EC/OC) was quite constant with an average value of 0.3 both during summer and during winter. The concentration of particulate organic matter (POM) was determined by multiplying the OC concentration by 1.7, which is the average ratio of the mass of carbon-containing species to carbon mass assumed to be distributed between the fine and coarse modes with a ratio of 7/3 (Quinn et al., 2000; Putaud et al., 2000; Neusüß et al., 2000).

During summer the number of filters analysed for EC/OC (8) was lower than that of the IC filters (22). To extrapolate the EC/OC observations for the whole period the measured mean EC value obtained using the thermo-optical determination technique (0.44 μg m^{-3}) has been compared with the corresponding mean value (0.52 μg m^{-3}) determined using a particle soot absorption particle (PSAP) instrument operating during the whole campaign with a sampling resolution of 5 min. (r^2=0.71 between the two data sets if one value is excluded). Thus, based on the determined EC/OC ratio and the measured EC levels during the whole campaign using the PSAP (mean value of 0.66), mean OC concentrations during the campaign have been derived.

Thus it was attempted to obtain mass closure based on a comparison between the weighted mass and the measured total ionic, dust, EC and POM masses. Figure 25a,b reports the results of this comparison for both the summer and the winter campaign, and for both the coarse and the fine fraction. In the fine fraction SO_4^{2-} and OC are the two main constituents since they account for up to 38 and 16%, respectively. On the other hand no dominant constituent was found in the coarse mode. The agreement between the weighted and estimated mass is quite reasonable during summer. (The estimated mass was about 12% lower than the weighted mass; Figure 25a,b). On the other hand the discrepancy between weighted and calculated mass was higher during winter (up to 30%). Water and the uncertainty in the use of diagnostic ratios for the dust determination (Andreae et al., 2002) can account in part of the missing compounds.

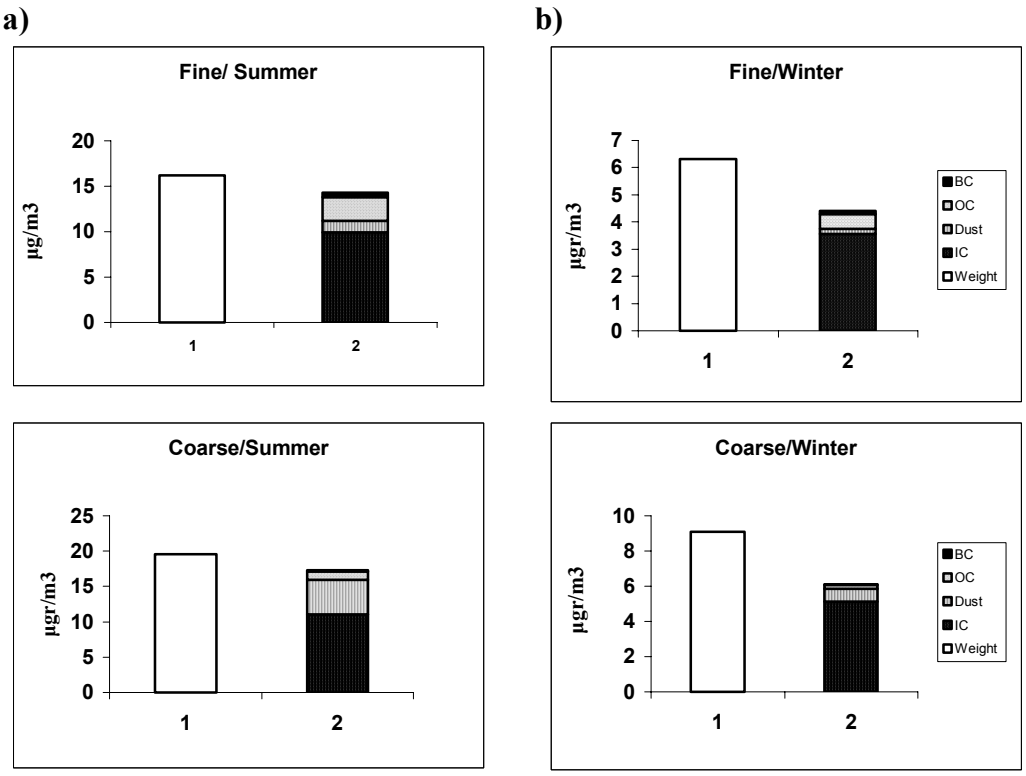

Figure 25: Mass closure based on a comparison between the weighted mass on the one hand and the measured total ionic mass, dust, EC and POM mass for both coarse and fine fractions and for both summer (25a) and winter campaigns (25b) respectively.

5.6 Mass closure

To estimate the inorganic fraction of particulate matter we have assumed the most likely chemical species for each element to be SO_4^{2-}, NO_3^-, Cl^-, NH_4^+, Na^+, Mg^{2+}, Br, $CaCO_3$, K_2CO_3, TiO_2, Fe_2O_3, Al_2O_3, SiO_2, SrO, MnO, ZnO, PbO, NiO, CuO, Cr_2O_3, and V_2O_5 . Here we used results from IC analysis showing that the major fraction of the fine particle mass is composed of ammonium sulphate and bisulphate and that nitrate and chloride in the coarse fraction are practically counterbalanced by sodium and magnesium. Further, for potassium we assumed carbonate as a product of biomass burning, although chloride and sulphate in the fine fraction (Christensen and Livbjerg, 2000) and soil-derived oxide in the coarse mode should also be considered. The mass balance has been investigated both for the fine (PM_1) and for the coarse (PM_{10}-PM_1) particle mode. The results, presented as a ratio of inorganic mass determined by IC and PIXE and total mass obtained from gravimetry, are shown in Figure 26a–Figure 26c. As can be seen the inorganic fraction accounts for about 60% of the coarse particle mass and for 35-120% of the fine particle mass collected during the summer campaign.

The results from the boat campaign are comparable – inorganic substances, again, account on average for 60% of the coarse particle mass and for 65-80% of the fine particle mass. During winter inorganic substances contribute about 45-80% to the coarse particle fraction (on average about 60%) and between 50 to 90% to the fine the particle fraction.

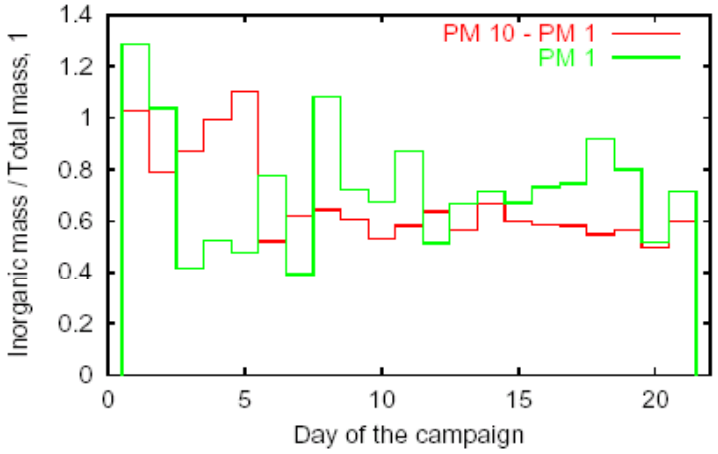

Figure 26a: Ratio of inorganic to total mass concentrations for PM_1 and (PM_{10}-PM_1) fractions collected at Finokalia 10–31 July 2000.

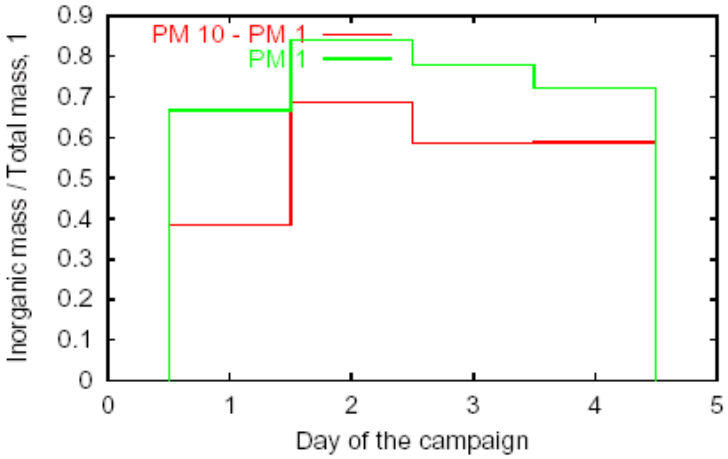

Figure 26b: Ratio of inorganic to total mass concentrations for PM_1 and (PM_{10}-PM_1) fractions collected aboard the research vessel "AEGAIEO" 25–29 July 2000.

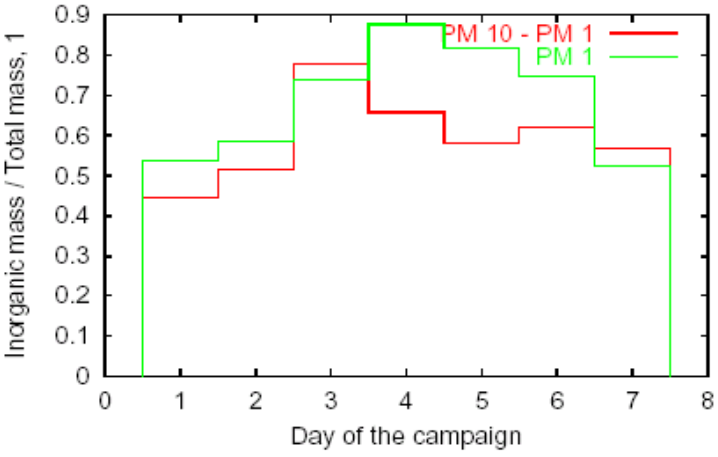

Figure 26c: Ratio of inorganic to total mass concentrations for the PM_1 and the (PM_{10}-PM_1) fractions collected at Finokalia 7–14 January 2001.

One of the aims of the measurement campaign was to measure key aerosol and gaseous species over the Mediterranean Sea and within an air mass that would later reach the Finokalia sampling site, where the same parameters were measured in parallel. For this reason measurements were performed also aboard the research vessel "AEGAIO". It was essential that samples collected at the two platforms were taken from the same air masses, and that the time lag between the two measurements were known. The course of the vessel was continuously adjusted to follow the relevant air mass movement according to the forecast. A trip of about six hours was required on the first day in order to reach the area of interest according to the forecast. During the following three days course tracking was successfully performed. Subsequent analysis confirmed that for the 6-hour interval trajectories received on board there was satisfactory agreement of position and time between the forecast trajectory and the vessel course.

5.7 Conclusions

Determination of the chemical composition of aerosols has been performed in size-resolved atmospheric aerosol samples collected with a Berner low-pressure impactor during two campaigns conducted at a coastal site in the Eastern Mediterranean in the framework of the EU funded SUB-AERO project in July 2000 and January 2001.

The results from the measurement campaigns show that the eastern Mediterranean basin is moderately to highly polluted during the summer and relatively unpolluted during the winter. Elevated pollutant loadings in summer result from stable meteorological conditions and the absence of wet removal mechanisms. In addition, black carbon contributions from extensive forest fires occurring within the Mediterranean region were also present during the summer campaign.

Optical and physical properties suggest that mineral dust (*e.g.* from the Sahara) and marine components (i.e. from sea spray) also contribute to aerosols in the eastern Mediterranean. Resuspension from soil also seems to be important for the aerosol size distribution at this location.

Sulphate is the main ion in the fine mode accounting for about 65% of the total ionic mass. Sulphate and NH_4^+ combined account for up to 90% of the total mass in the fine fraction. In the coarse mode there is no single dominant ion. The five ions Na^+, Cl^-, Ca^{2+}, CO_3^{2-} and NO_3^- exhibit almost equal concentrations and account for up to 90% of the total ionic mass in the coarse fraction.

It was attempted to obtain mass closure on the basis of a comparison between the weighed mass and the measured total ionic, dust, EC and POM masses. The agreement between the weighed and estimated masses is quite good during summer (discrepancy less than 12%). On the other hand, the discrepancy between weighed and calculated masses during winter is larger (around 30%). Water may account for part of the missing mass, especially in the coarse mode.

In summary the aerosol monitoring campaigns at Finokalia suggest that the site is significantly influenced by aged pollution plumes produced from upwind source regions located within Western Europe, sea salt, resuspended dust, and in some occasions from Saharan dust episodes.

Acknowledgments

We thank the European Commission, Environment and Climate Programme, (EVK2-CT-1999-000052 Acronym: SUB-AERO) for financial support.

6. References

Andreae, T.W., Andreae, M.O., Ichoku, C., Maenhaut, W., Cafmeyer, J., Karnieli, A., and Orlovsly, L. (2002) Light scattering by dust and anthropogenic aerosol at a remote site in the Negev desert, Israel. *J. Geophys. Res., 107*, 252-290.

Birch, M.E. and Cary, R.A. (1996) Elemental carbon-based method for monitoring occupational exposures to particulate diesel exhaust. *Aerosol Sci. Technol., 23,* 221-241.

CEN (1998) Air Quality. Determination of the PM10 fraction of suspended particulate matter. Reference method and field test procedure to demonstrate reference equivalence of measurement methods. Brussels, European Committee for Standardization (European Standard EN 12341).

Christensen, K.A. and Livbjerg, H. (2000) A plug flow model for chemical reactions and aerosol nucleation and growth in an alkali-containing flue gas. *Aerosol Sci. Technol., 33*, 470-489.

Dockery, D.W., Pope, C.A. III, Xu, X., Spengler, J.D., Ware, J.H., Fay. M.E., Ferris, B.G. Jr. and Speizer, F. E. (1995). An association between air pollution and mortality in six U.S. cities. *N. Engl. J. Med., 329*, 1753-1759.

EMEP (2001) Transboundary particulate matter in Europe: status report 2001. Eds: Lazaridis, M., Tarrason, L., Tørseth, K. Kjeller, Norwegian Institute for Air Research (EMEP Report 4/2001).

EMEP/CCC (1996) Manual for sampling and chemical analyses. Kjeller, Norwegian Institute for Air Research (EMEP/CCC Report 1/95).

EMEP/CCC (2001) Measurement of particulate matter in EMEP. Ed: Lazaridis, M. Kjeller, Norwegian Institute for Air Research (EMEP/CCC-Report 5/2001).

Finlayson-Pitts, B. J. and Pitts, J. N., Jr. (2000) Chemistry of the upper and lower atmosphere, theory, experiments, and applications. San Diego, Academic Press. Chapt. 9.

Haulet, R., Zettwoog, P. and Sabroux, J.C. (1977) Sulphur dioxide discharge from Mount Etna. *Nature, 268*, 715-717.

Havránek, V., Hnatowicz, V. Kvítek, J. and Obrusník, I. (1994) PIXE-INP computer code for analyses of thin and thick samples. *Nucl. Instr. Meth., B85*, 637-641.

Havránek, V., Kučera, J., Horáková, J., Voseček, V., Smolík, J., Schwarz, J. and Sýkorová, I. (1999) Matrix effects in PIXE analysis of aerosols and ashes. *Biological Trace Elements Research, 71-72*, 431-442.

Hillamo, R. E. and Kaupinnen, E. I. (1991) On the performance of the Berner low pressure impactor. *Aerosol Sci. Technol., 14*, 33-47.

Hillamo, R. E., Makela, T., Schwarz, J. and Smolík, J. (1999) Collection characteristics of the model 25/0,018/2 Berner low pressure impactor. *J. Aerosol Sci., 30(S1),* 901-902.

Horvath, H., Kasahara, M. and Pesava, P. (1996) The size distributions and composition of the atmospheric aerosol at a rural and nearby urban location. *J. Aerosol Sci.*, *27*, 417-435.

Jakobsen, M.C., Hansson, H.-C., Noone, K.J. and Charlson, R.J. (2000) Organic atmospheric aerosols: review and state of the science. *Rev. Geophys., 38*, 267-294.

Kirchstetter, T. W., Corrigan, C. E. and Novakov, T. (2001) Laboratory and field investigation of the adsorption of gaseous organic compounds onto quartz filters. *Atmos. Environ., 35*, 1663-1671.

Lazaridis, M., Semb, A., Larssen, S., Hjellbrekke, A.-G., Hov, Ø., Hanssen, J. E., Schaug, J. and Tørseth, K. (2002) Measurements of particulate matter within the framework of the European Monitoring and Evaluation Programme (EMEP) I. First results. *Sci. Total Environ., 285*, 209-235.

Liu, B. Y. H. and Pui, D. Y. H. (1981) Aerosol sampling inlets and inhalable particles. *Atmos. Environ, 15*, 589-600.

Mäkelä, J.M., Yli-Koivisto, S., Hiltunen, V., Mattila, T., Koponen, I.K., Teinilä, K. and Hillamo, R. (2000) Aerosol particle mass collection in BIOFOR. In: *Biogennic Aerosol Formation in the Boreal Forest (BIOFOR). Final report, EC Environment & Climate Research Programme (Oct. 1997 – Sept. 1999).* Eds: M. Kulmala and K. Hämeri. Helsinki, Finnish Association for Aerosol Research (Report Series in Aerosol Science No.47).

Mason, B. and Moore, C.B. (1982) Principles of geochemistry, 4th ed. New York, John Wiley & Sons.

McDow, S. R. and Huntzicker, J. J. (1990) Vapor adsorption artifact in the sampling of organic aerosol: face velocity effects. *Atmos. Env., A 24*, 2563-2571.

Neusüß, C., Pelzing, M., Plewka, A., Hermann, H. (2000) A new analytical approach for size-resolved speciation of organic compounds in atmospheric aerosols particles: methods and first results. *J. Geophys. Res., 105*, 4513-4527.

Nicholson, K.W. (1988) A review of particle resuspension. *Atmos. Environ., 22*, 2639-265.

NIOSH (1994) NIOSH Manual of Analytical methods (NMAM), 4th ed., method 5040. Cincinnati, National Institute for Occupational Safety and Health.

NOAA Air Resources Laboratory (2001) http://www.arl.noaa.gov/ready/hysplit4.html

Ondov, J.M., Biremann, A.H., Heft, R.E. and Koszykowski, R.F. (1981) Atmospheric aerosol source/air quality relationships: elemental composition of atmospheric fine particles emitted from coal burned in a modern power plant equipped with flue gas desulfurisation system. *ACS Symp. ser., 161*, 173-187.

Pandis, S.N., Paulson, S.E., Seinfeld, J.H. and Flagan, R.C. (1991) Aerosol formation in the photooxidation of isoprene and B-pinene. *Atmos. Environ., A 25*, 997-1008.

Pope, C.A., Dockery, D.W. and Schwartz, J. (1995) Review of epidemiological evidence of health-effects of particulate air pollution. *Inhal. Toxicol., 7*, 1-18.

Pope, C.A. III, Schwartz, J. and Ransom, M.R. (1995) Particulate air pollution as a prediction of mortality in a prospective study of US adults. *Am. J. Crit. Care Med., 151*, 669-674.

Pósfai, M. and Molnár, Á. (2000) Aerosol particles in the troposphere: a mineralogical introduction. In: *EMU notes in mineralogy, Vol. 2.* Eds.: Vaughan, D.J. and Wogelius, R.A. Budapest, Eötvös University Press, chapt. 6.

Putaud, J.P., Van Dingenen, R., Mangoni, M., Virkkula, A., Raes, F., Maring, H., Prospero, J.M., Swietlicki, E., Berg, O.H., Hillamo, R. and Makela, T. (2000) Chemical mass closure and assessment of the origin of the submicron aerosol in the marine boundary layer and the free troposphere at Tenerife during ACE. *Tellus, 52B*, 141-168.

Quinn, P.K., Bates, T.S., Coffman, D.J., Miller, T.L., Johnson, J.E., Covert, D.S., Putaud, J.P., Neususs, C. and Novakov, T. (2000) A comparison of aerosols chemical and optical properties from the first and the second aerosol characterization experiment. *Tellus, 52B*, 239-257.

Rahn, K.A., Borys, R.D., Shaw, G.E. Schütz, L. and Jaenicke, R. (1979) Long range impact of desert aerosol on atmospheric chemistry: two examples. In: *Saharan dust: mobilization, transport, deposition*. *Scope, 14*. Ed: C. Morales. Chichester, Wiley and Sons. pp. 244-266.

Savoie, D.L. and Prospero, J.M. (1982) Particle size distribution of nitrate and sulfate in the marine atmosphere. *Geophys. Res. Lett., 9*, 1207-1210.

Schlesinger, R.B. (1995) Toxicological evidence for health effects from inhaled particulate pollution. Does it support the human experience? *Inhal. Toxicol., 7,* 99-110.

Schütz, L. and Rahn, K.A. (1982) Trace element concentrations in erodible soils. *Atmos. Environ., 16*, 171-176.

Seaton, A., MacNee, W., Donaldson, K. and Godden, D. (1995) Particulate air pollution and acute health effects. *Lancet, 345*, 176-178.

Turpin, B. J., Huntzicker, J. J. and Hering S. V. (1994) Investigation of organic aerosol sampling artefacts in the Los Angeles basin. *Atmos. Environ., 28*, 3061-3071.

WHO (2000) Guidelines for Air Quality. Geneva, World Health Organization.

Wolfenbarger, J.K. and Seinfeld, J.H. (1990) Inversion of aerosol size distribution data. *J. Aerosol Sci.*, *21*, 227-247.

Appendix A

Time series of particulate matter concentrations ($\mu g/m^3$) at EMEP stations (2000)

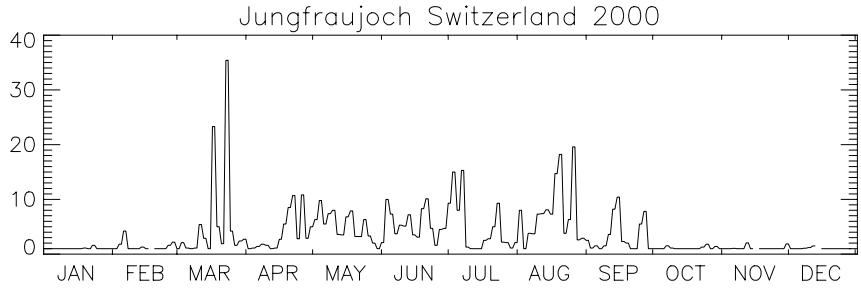
Jungfraujoch Switzerland 2000
40
30
20
10
0
JAN FEB MAR APR MAY JUN JUL AUG SEP OCT NOV DEC

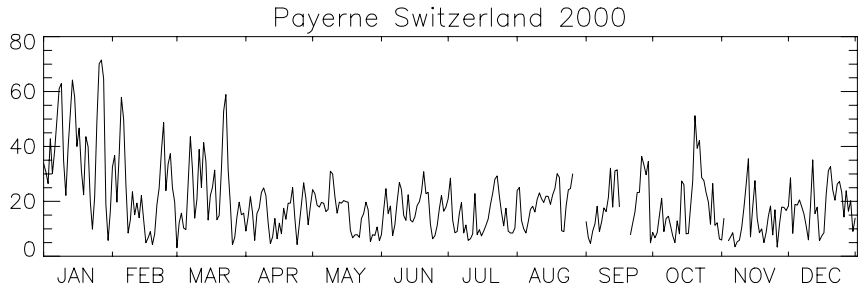
Payerne Switzerland 2000
80
60
40
20
0
JAN FEB MAR APR MAY JUN JUL AUG SEP OCT NOV DEC

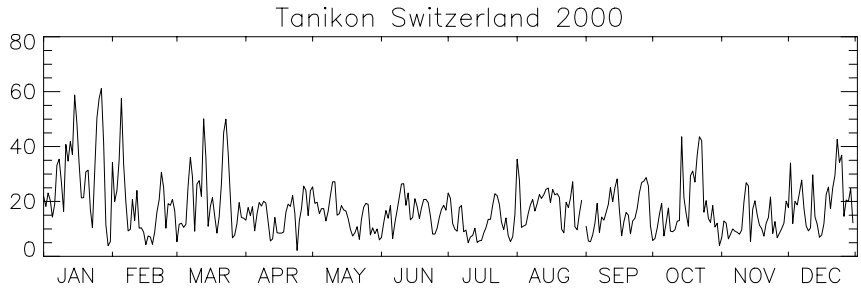
Tanikon Switzerland 2000
80
60
40
20
0
JAN FEB MAR APR MAY JUN JUL AUG SEP OCT NOV DEC

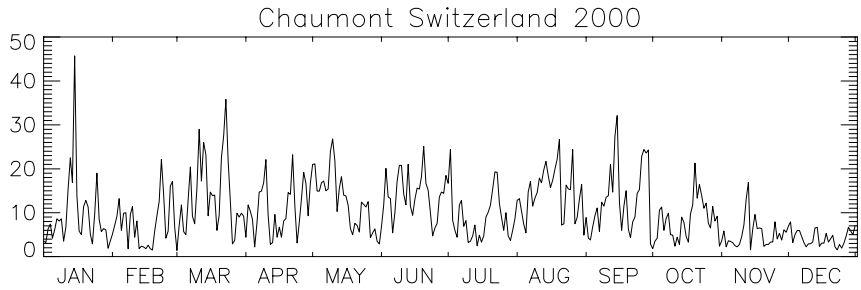
Chaumont Switzerland 2000
50
40
30
20
10
0
JAN FEB MAR APR MAY JUN JUL AUG SEP OCT NOV DEC

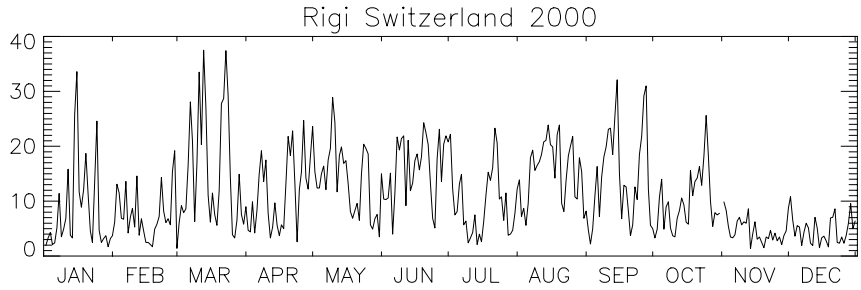
Rigi Switzerland 2000
40
30
20
10
0
JAN FEB MAR APR MAY JUN JUL AUG SEP OCT NOV DEC

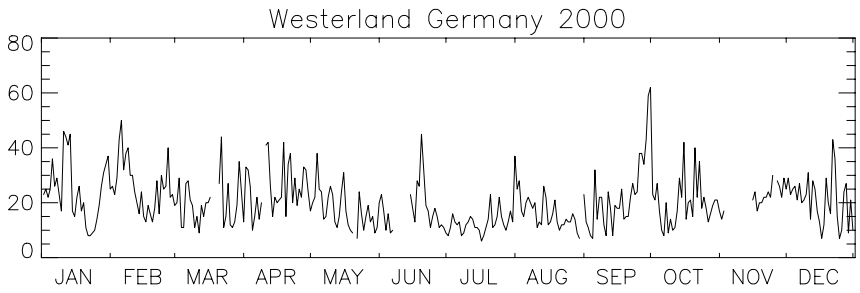
Westerland Germany 2000
80
60
40
20
0
JAN FEB MAR APR MAY JUN JUL AUG SEP OCT NOV DEC

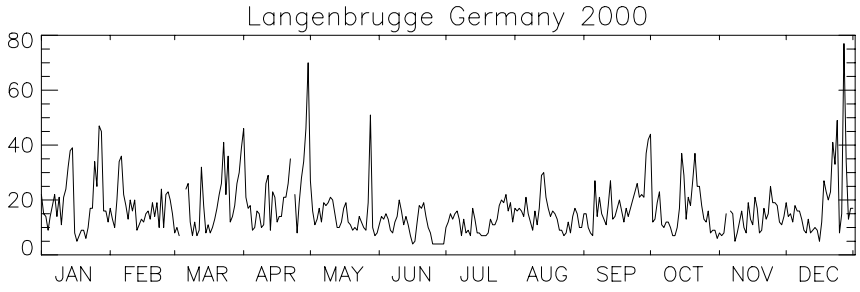
Langenbrugge Germany 2000
80
60
40
20
0
JAN FEB MAR APR MAY JUN JUL AUG SEP OCT NOV DEC

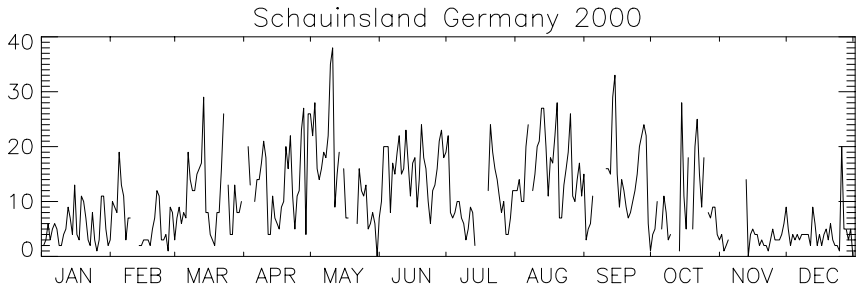
Schauinsland Germany 2000
40
30
20
10
0
JAN FEB MAR APR MAY JUN JUL AUG SEP OCT NOV DEC

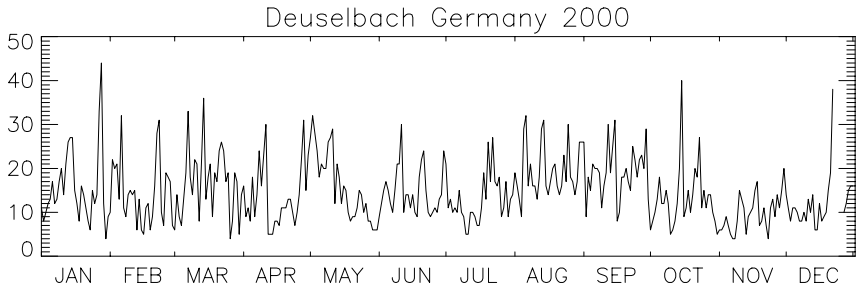
Deuselbach Germany 2000
50
40
30
20
10
0
JAN FEB MAR APR MAY JUN JUL AUG SEP OCT NOV DEC

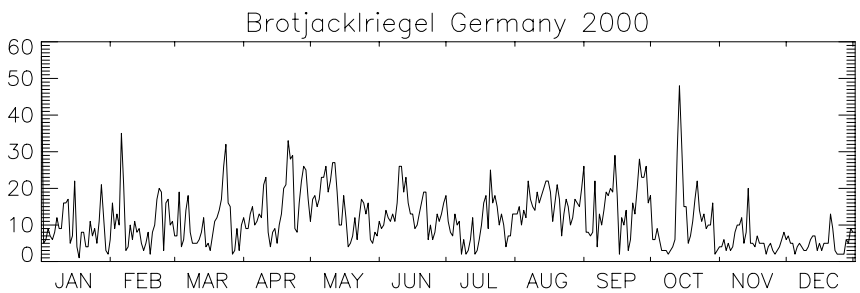
Brotjacklriegel Germany 2000
60
50
40
30
20
10
0
JAN FEB MAR APR MAY JUN JUL AUG SEP OCT NOV DEC

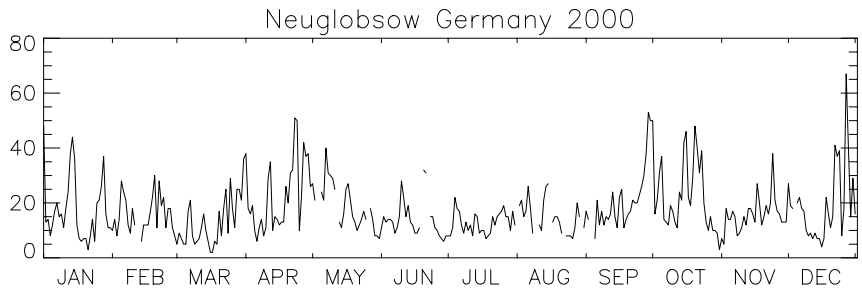
Neuglobsow Germany 2000
80
60
40
20
0
JAN FEB MAR APR MAY JUN JUL AUG SEP OCT NOV DEC

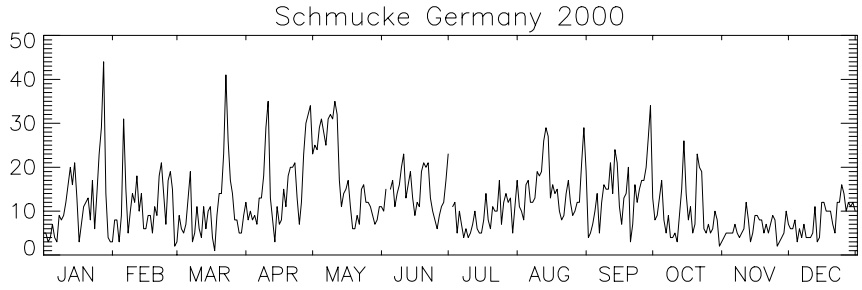
Schmucke Germany 2000
50
40
30
20
10
0
JAN FEB MAR APR MAY JUN JUL AUG SEP OCT NOV DEC

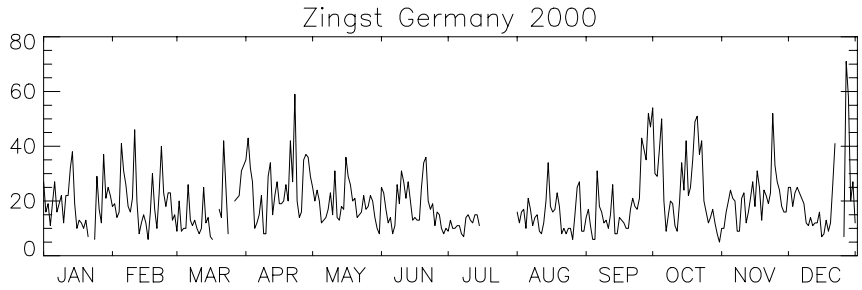
Zingst Germany 2000
80
60
40
20
0
JAN FEB MAR APR MAY JUN JUL AUG SEP OCT NOV DEC

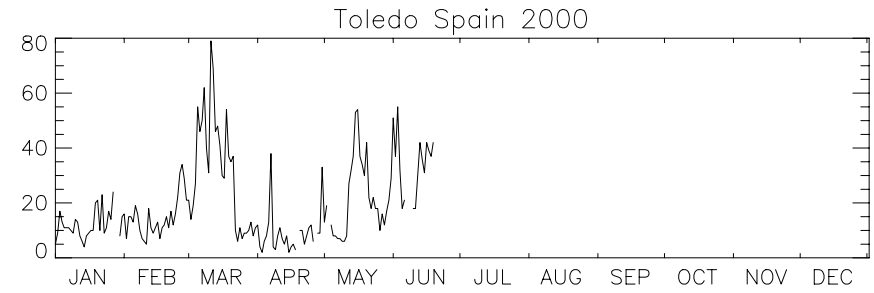
Toledo Spain 2000
80
60
40
20
0
JAN FEB MAR APR MAY JUN JUL AUG SEP OCT NOV DEC

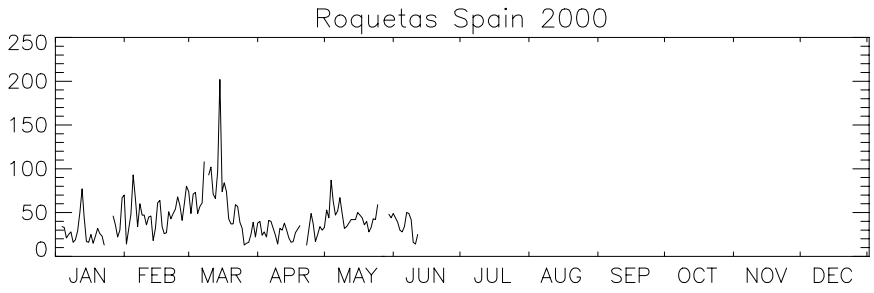
Roquetas Spain 2000
250
200
150
100
50
0
JAN FEB MAR APR MAY JUN JUL AUG SEP OCT NOV DEC

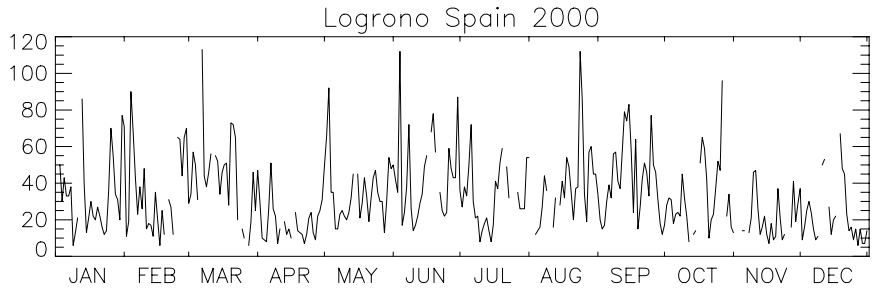
Logrono Spain 2000
120
100
80
60
40
20
0
JAN FEB MAR APR MAY JUN JUL AUG SEP OCT NOV DEC

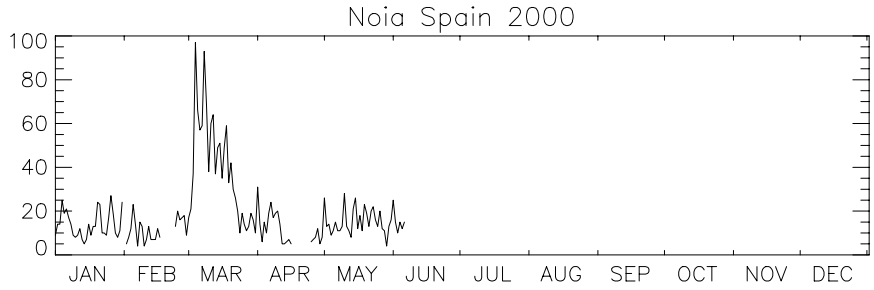
Noia Spain 2000
100
80
60
40
20
0
JAN FEB MAR APR MAY JUN JUL AUG SEP OCT NOV DEC

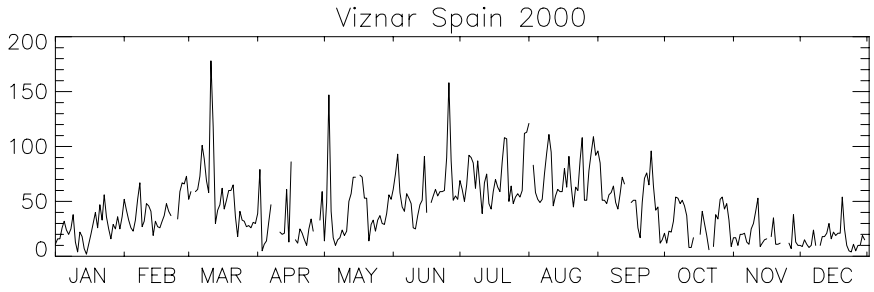
Viznar Spain 2000
200
150
100
50
0
JAN FEB MAR APR MAY JUN JUL AUG SEP OCT NOV DEC

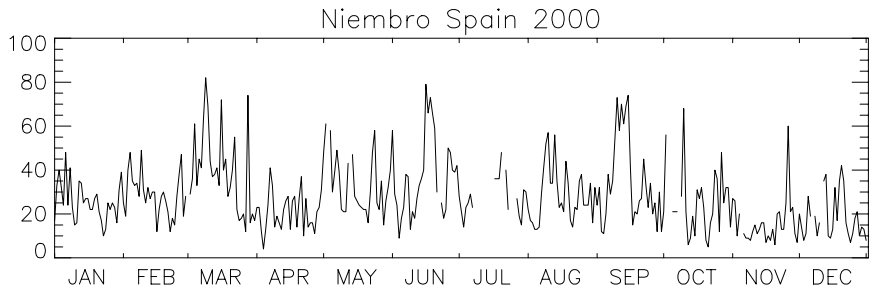
Niembro Spain 2000
100
80
60
40
20
0
JAN FEB MAR APR MAY JUN JUL AUG SEP OCT NOV DEC

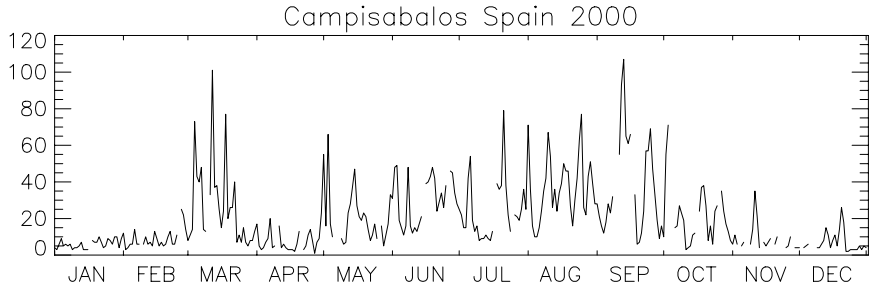
Campisabalos Spain 2000
120
100
80
60
40
20
0
JAN FEB MAR APR MAY JUN JUL AUG SEP OCT NOV DEC

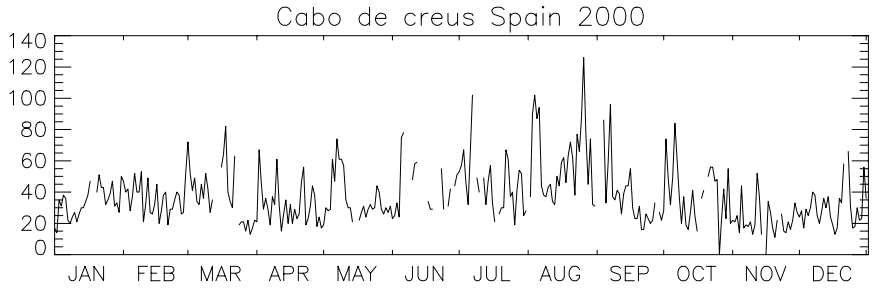
Cabo de creus Spain 2000
140
120
100
80
60
40
20
0
JAN FEB MAR APR MAY JUN JUL AUG SEP OCT NOV DEC

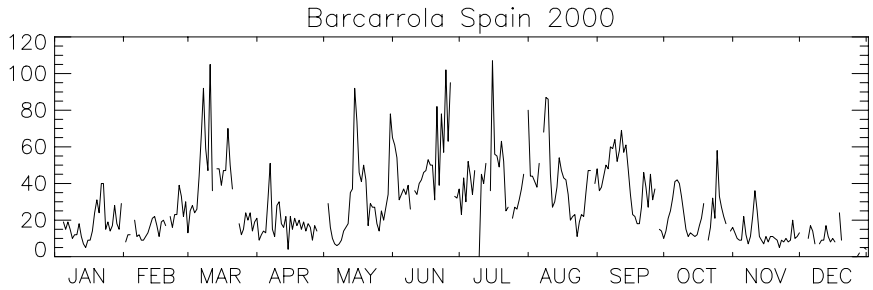
Barcarrola Spain 2000
120
100
80
60
40
20
0
JAN FEB MAR APR MAY JUN JUL AUG SEP OCT NOV DEC

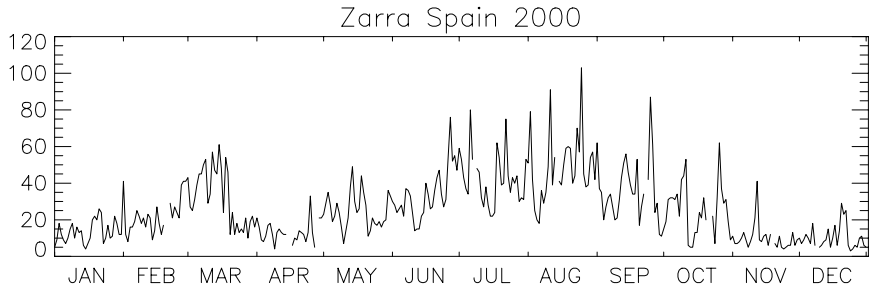
Zarra Spain 2000
120
100
80
60
40
20
0
JAN FEB MAR APR MAY JUN JUL AUG SEP OCT NOV DEC

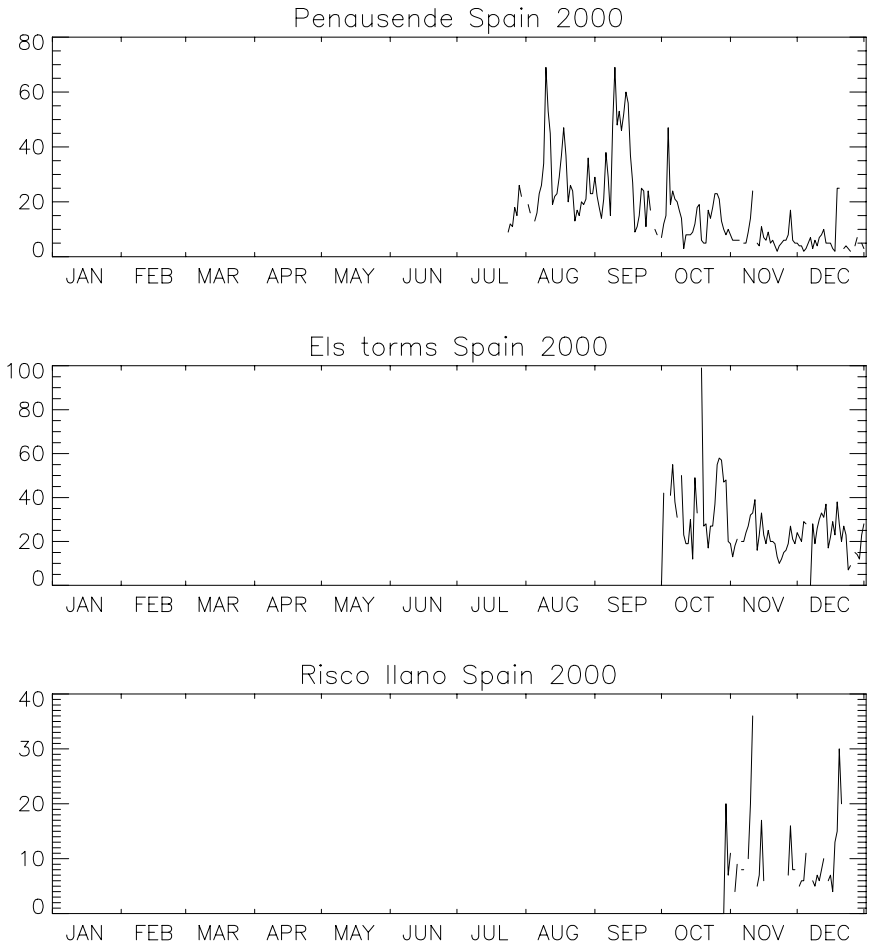
Penausende Spain 2000
80
60
40
20
0
JAN FEB MAR APR MAY JUN JUL AUG SEP OCT NOV DEC
Els torms Spain 2000
100
80
60
40
20
0
JAN FEB MAR APR MAY JUN JUL AUG SEP OCT NOV DEC
Risco llano Spain 2000
40
30
20
10
0
JAN FEB MAR APR MAY JUN JUL AUG SEP OCT NOV DEC